JOURNAL OF QUATERNARY SCIENCE (2022) 1–27 ISSN 0267-8179. DOI: 10.1002/jqs.3433

JQS Journal of Quaternary Science QRA Quaternary Research Association

Last interglacial lake sediments preserved beneath Laurentide and Greenland Ice sheets provide insights into Arctic climate amplification and constrain 130 ka of ice-sheet history

GIFFORD H. MILLER,[1]* ALEXANDER P. WOLFE,[2] YARROW AXFORD,[3] JASON P. BRINER,[4] HELGA BUELTMANN,[5] SARAH CRUMP,[6,7] DONNA FRANCIS,[8] BIANCA FRÉCHETTE,[9] DEVON GORBEY,[4] MEREDITH KELLY,[10] JAMIE MCFARLIN,[11] ERICH OSTERBERG,[10] JONATHAN RABERG,[12] MARTHA RAYNOLDS,[13] JULIO SEPÚLVEDA,[1] ELIZABETH THOMAS[4] and GREGORY DE WET[14]

[1]INSTAAR and Department of Geological Sciences, University of Colorado Boulder, Boulder, CO, USA
[2]Department of Geography, University of Manitoba, Winnipeg, MB, Canada
[3]Department of Earth & Planetary Sciences, Northwestern University, Evanston, IL, USA
[4]Department of Geology, University at Buffalo, Buffalo, NY, USA
[5]Institute of Biology and Biotechnology of Plants, University of Münster, Münster, Germany
[6]Genomics Institute, University of California Santa Cruz, Santa Cruz, CA, USA
[7]Institute of Arctic and Alpine Research, University of Colorado Boulder, Boulder, CO, USA
[8]Department of Geosciences, University of Massachusetts, Amherst, MA, USA
[9]GEOTOP, Université du Québec à Montréal, Montréal, Québec, Canada
[10]Department of Earth Sciences, Dartmouth College, Hanover, NH, USA
[11]Department of Geological Sciences, University of Colorado Boulder, Boulder, CO, USA
[12]INSTAAR and Department of Geological Sciences, University of Colorado Boulder, Boulder, CO, USA
[13]Institute of Arctic Biology, University of Alaska Fairbanks, Fairbanks, AK, USA
[14]INSTAAR, University of Colorado Boulder, and Geosciences, Smith College, Northampton, MA, USA

Received 7 April 2021; Revised 24 April 2022; Accepted 26 April 2022

ABSTRACT: Sediment cores from 13 lakes in a 1500 km transect along the eastern North American Arctic contain up to four superposed stratified interglacial units. All 13 lakes contain one unit with sediment similar in character and mass to Holocene gyttja, with ^{14}C ages >40 ka, luminescence ages 90 to 120 ka, and pollen assemblages that require nearly complete Laurentide deglaciation, supporting a Last Interglacial (LIG; MIS 5e) age. Two lakes preserve an older interglacial, with luminescence ages suggesting an MIS 7 age. Four adjacent lakes record a thin, stratified organic unit between the LIG and Holocene units with ^{14}C ages >50 ka, that is probably from late in MIS 5. Temperature estimates from biotic proxies suggest LIG summer temperatures 4–6°C above mid-20th century values; pollen, chironomids and DNA document a poleward expansion of woody plants and invertebrate species during the LIG, supporting arguments that positive feedbacks native to the Arctic amplified insolation-driven summer temperature increases. The stratigraphic succession implies the Laurentide Ice Sheet remained intact with sea level below -40 m from ~115 ka to ~11 ka, and places new constraints on the interpretation of cosmogenic radionuclide inventories in erratic boulders older than the Holocene throughout this region. © 2022 John Wiley & Sons, Ltd.

KEYWORDS: Arctic; Arctic amplification; Baffin Island; lakes; Last Interglacial

Introduction

As the planet warms under increasing anthropogenic greenhouse gas forcing, the Arctic is warming at three times the global rate (AMAP 2021). There is increasing interest in how the Arctic terrestrial environment will respond to greater summer warmth, and whether positive feedbacks beyond those linked directly to cryospheric losses via albedo effects will continue to amplify warming into the future. For example, documented contemporary shrub tundra expansion and Arctic 'greening' may have a considerable effect on local and regional albedos (Myers-Smith *et al.* 2020).

Reconstructions of ecosystem status in past warm times when continental configurations were similar to the present offer an opportunity to inform expectations of changes likely to occur in the near future. Past orbitally driven Northern Hemisphere summer insolation maxima resulted in an early Holocene thermal maximum (*ca.* 10 to 5 ka). Even stronger orbitally forced summer insolation anomalies occurred during the Last Interglacial (LIG; MIS 5e *ca.* 130 to 115 ka), with peak summer insolation at 65°N 12% higher than the present at 129 ka, whereas the Holocene peak summer insolation anomaly was 9% higher than the present at 11 ka (Berger, 1978). Additionally, unlike the last deglaciation, MIS 6 deglaciation was complete and the sea level close to the present by the time of peak summer insolation (129 ka; McCulloch and Esat, 2000), whereas Holocene deglaciation resulted in the sea level not reaching modern levels until ~6ka, ~5 kyr after the insolation maximum (Fig. 1). As a result, the full strength of the LIG positive summer insolation anomaly was available to warm the Arctic instead of being consumed melting ice. This probably resulted in significantly greater summer warming and more substantial retreat of the Arctic cryosphere during the Last Interglacial than at any time in the Holocene, but these changes are only sparsely documented globally.

*Correspondence: G.H. Miller, as above.
E-mail: gmiller@colorado.edu

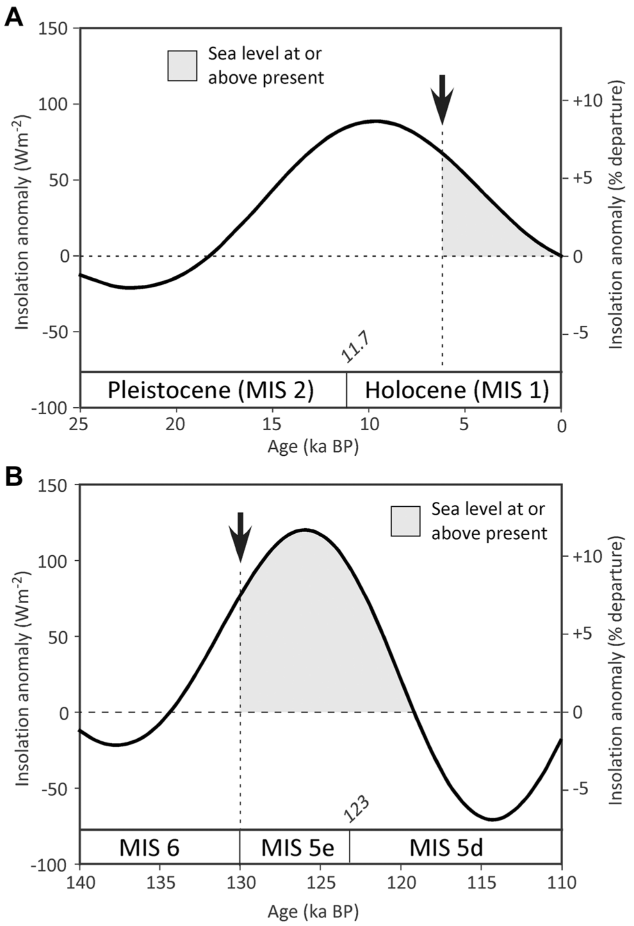

Figure 1. July insolation anomalies for 0–25 ka (upper panel) and 110–140 ka (lower panel) with bold arrow denoting the date at which sea level reached close to present following MIS 2 deglaciation (upper panel) and MIS 6 deglaciation (lower panel). The solar energy contributing to summer warmth of the Last Interglacial greatly exceeds that of the Holocene due to a combination of earlier deglaciation in the precession cycle and the alignment of the obliquity and precession terms to produce a greater summer insolation anomaly.

Continuous records of LIG environments have been reported for Arctic regions outside the limits of the Pleistocene ice sheets, including lakes in Beringia (Lozhkin and Anderson, 1995; Melles *et al.* 2012; Brigham-Grette *et al.* 2013), in marine sediment cores containing terrestrial material (de Vernal and Hilaire-Marcel, 2008; Cluett and Thomas, 2021) and in permafrost cryostratigraphy. However, from the glaciated regions, including northeastern North America and Greenland, stratified terrestrial LIG sediments are exceptionally rare. Over the past several decades our teams have recovered stratified lacustrine sediment below Holocene gyttja with ^{14}C ages >40 ka in lake basins over a 1500 km transect along northeastern North American coastal margins. Luminescence indicates that the thickest, most prominent pre-Holocene unit was deposited during MIS 5, and a range of biotic proxies preserved in that unit, primarily pollen (Fréchette *et al.* 2006), midges (Francis *et al.* 2006; Axford *et al.* 2011; McFarlin *et al.* 2018) and DNA (Crump *et al.* 2021) indicate summers warmer than at any time in the Holocene and that require the Laurentide and Greenland ice sheets to be as small as, or smaller, than today. With this evidence we interpret these units to have been deposited during the Last Interglacial, MIS 5e.

In this paper we review the setting, stratigraphy, geochronology, and palaeoclimate inferences of the interglacial units from 12 lakes with stratified interglacial sediment over a 1200 km south–north transect along eastern Baffin Island in the Eastern Canadian Arctic and one lake in northwest Greenland (Fig. 2). Details for six of these lakes (Robinson Lake (RL), Amarok Lake (AKL), Fog Lake (FOG), Brother of Fog Lake (BRO), CF8 and Wax Lips Lake (WLL)) have been published previously; four (Lake Attata (ATA), Drop Lake (DRP), Spot Lake (SPT) and Africa Lake (AFR)) are published here for the first time; and three others (Saddle Lake (SAD), Gnarly Lake (GNR) and Canso Lake (CAN)) are only briefly mentioned in previous publications. The Baffin Island lakes lay beneath the Laurentide Ice Sheet (LIS) at the Last Glacial Maximum (LGM), but, with the exception of SAD, the lake sediment in their central deeps never froze.

Taken as a whole, the records from these lakes provide key constraints not only on the climate differences between present and earlier interglacials, but also on the dimensions of the Laurentide and Greenland ice sheets across the last glacial cycle. New constraints on ice-sheet dimensions allow us to revisit the interpretation of cosmogenic inventories in erratic boulders in the regions of our lake records. Summer temperature proxies identify interglacial times warmer than peak Holocene warmth and biotic remains provide predictive evidence for the likely evolution of ecosystem status as the Arctic continues to warm. The commonalities in stratigraphic preservation across these 13 lakes also allows us to revisit the interpretation of conflicting radiocarbon ages in clastic sediment deposited immediately preceding Holocene gyttja in many lakes.

Because there is a high probability that many other lakes in Arctic Canada and Greenland situated in favourable topographic settings preserve pre-Holocene stratified interglacial sediment, we summarise the characteristics shared by the 13 lakes reported here (see below, 'Optimal characteristics for preservation of ancient sediment in lakes beneath continental ice sheets'), to provide guidelines that may aid future researchers interested in such records.

Preservation of ancient landscapes beneath continental ice sheets

Continental glaciation eroded most extant lakes and created new lakes, but for lakes in landscapes that experienced only cold-based glaciation, preservation of preglacial landscapes is plausible. Sugden (1978) utilised satellite imagery to quantify patterns of glacial erosion under the LIS as indices of basal thermal regime, modulated by topography. He showed that in cold regions of high topographic relief, ice velocities varied spatially with bed topography, resulting in localised regions experiencing limited or no glacial erosion, thereby affording the potential for preservation of ancient landscapes, including lake sediments (Fig. 3). The low-relief uplands and coastal lowlands of eastern Baffin Island exhibit little sign of glacial erosion, an interpretation supported by interbedded marine and glacial units of early to late Pleistocene age exposed in coastal cliffs along the Clyde (Feyling-Hanssen, 1976; Refsnider *et al.* 2013) and Qivitu (Nelson, 1982) forelands. Ancient surficial features, such as the 82 km^2 Cape Aston Delta and associated 80 m asl shoreline traceable for over 25 km dated to >50 ka (Løken 1966) are consistent with limited erosion in coastal regions. Erratic boulders on the Cape Aston Delta have cosmogenic exposure ages indicating deposition by cold-based Laurentide ice during the LGM (Davis *et al.* 2006), confirming overriding by cold-based LGM ice without erosion. Comparable geological evidence from northwest Greenland

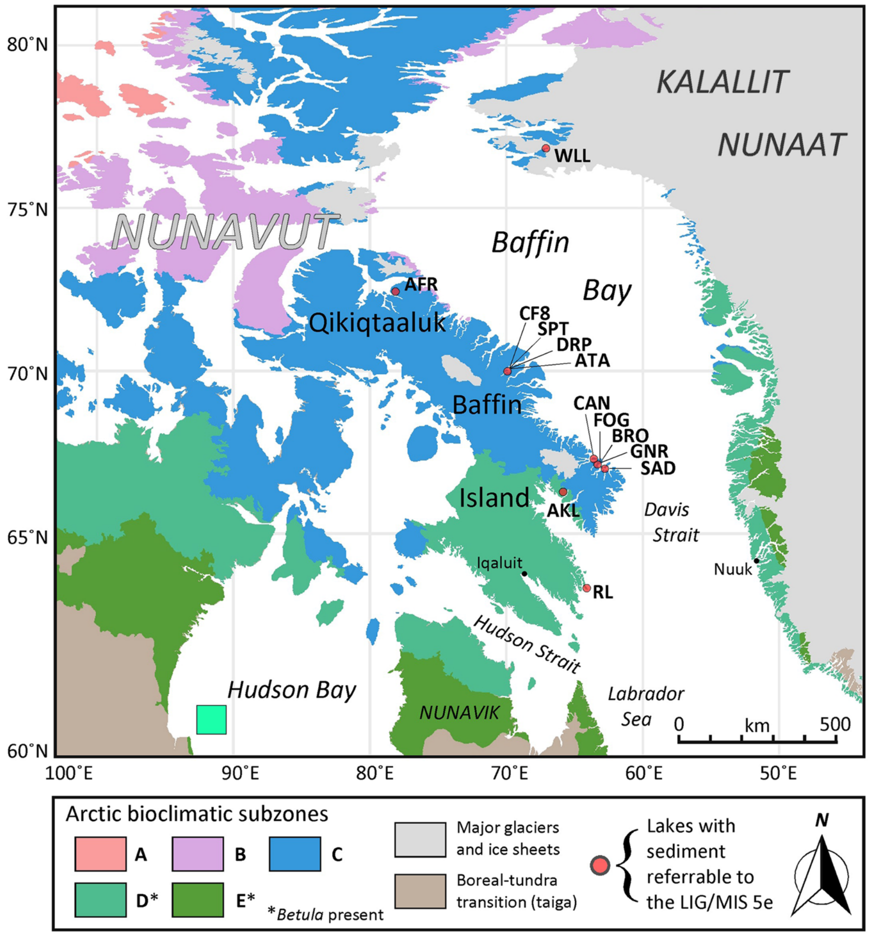

Figure 2. Map of northeast North American Arctic, showing the location of lakes with stratified Last Interglacial sediment discussed in the text, overlying the contemporary bioclimatic subzones. Iqaluit is the capital city of Nunavut. [Color figure can be viewed at wileyonlinelibrary.com]

indicates cold-based LGM ice cover and similar preservation of pre-LGM landscapes in some settings (Bennike and Böcher, 2021; Kelly *et al.* 1999, Corbett *et al.* 2016, Farnsworth *et al.* 2018). Widespread evidence demonstrating landscapes inundated by both Laurentide and Greenland ice sheets remained unmodified by the overriding ice, opens the possibility that lacustrine sediment might be preserved over multiple glacial cycles (Fig. 4).

Conceptual model of Arctic lake sedimentation through a glacial–interglacial cycle

We postulate that lakes will *always* experience sedimentation if they are at least seasonally ice-free. A corollary is that if there is no deposition, the lake was either perennially frozen or beneath a cold-based glacier. The anticipated sedimentary record spanning interglacial–glacial–interglacial timeseries is diagrammed in Fig. 5. During interglaciations lakes are ice-free for a few months in summer, with tundra-vegetation stabilising unglaciated catchment soils, leading to gyttja-dominated sedimentation (Fig. 5A). As the climate shifts to 'glacial mode' lake ice no longer melts in summer, catchment vegetation dies back, expanding snowfields persist through summer until they merge with the advancing continental ice sheet; sedimentation ceases (Fig. 5B). During full glacial time (Fig. 5C), lake ice thickens but thermodynamics will not allow the lake to freeze completely, except in very shallow (<4 m depth) lakes, and there is no sedimentation. During deglaciation (Fig. 5D), summers are warm, glacial meltwater and snowmelt erode ancient unvegetated catchment soils, producing relatively high sedimentation rates of dominantly minerogenic sediment containing a variable mixture of ancient and contemporaneous proxies and organic carbon. The mass of newly deposited minerogenic sediment slowly dewaters the underlying gyttja, densifying the buried interglacial sediment. Once the ice sheet leaves the catchment, vegetation quickly stabilises catchment soils, reducing minerogenic input and resulting in gyttja sedimentation (Fig. 5E).

A conceptual sediment core from a lake that has experienced four discrete interglaciations following the sedimentation model described above is shown in Fig. 6. Gyttja units (hatched, odd numbers) are separated by minerogenic units (stippled, even numbers) deposited during deglaciation, after which gyttja deposition resumes. The three buried gyttja units have been dewatered by the weight of overlying minerogenic sediment, hence are 'compact organic' gyttja (e.g. Unit 5co). Magnetic susceptibility (MS) is always high in the minerogenic units, and low in the gyttja, which has high organic content (loss on ignition) and biogenic silica (diatoms). Model is based on Lake CF8 cores.

Methods

Lake sediment cores

The lake sediment cores were recovered using a hammer-driven piston corer and either polycarbonate, PVC, or aluminium core pipe, ranging from 63 to 110 mm internal diameter. A hammer-driven system is usually required as the

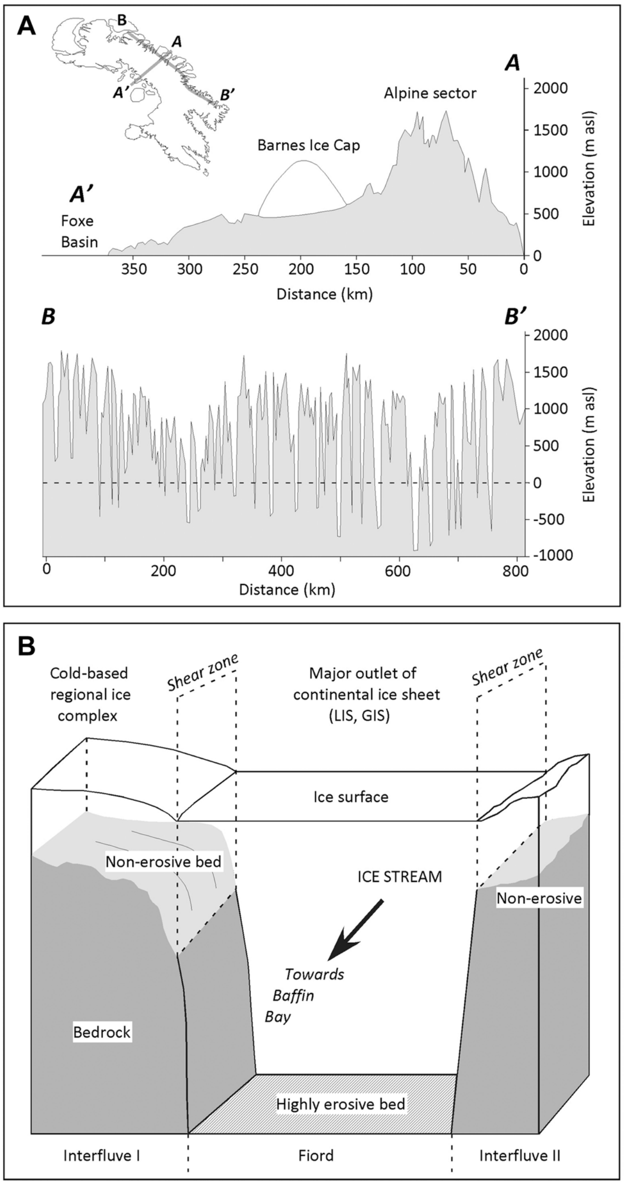

Figure 3. Baffin Island relief and its relation to variable conditions at the bed of the Laurentide Ice Sheet. A) topographic cross-section along A–A′ illustrating the Laurentide Ice Sheet blocking potential of the high mountains that form the eastern margin of Baffin Island (upper panel) and an elevation profile through the mountains along the east coast of Baffin Island (B–B′) showing the high-relief of the fjord systems that allowed localised rapid ice flow of Laurentide ice within the fjords, whereas ice was frozen at the bed over the interfluves. B) Cross-section of a Laurentide Ice Sheet outlet glacier flowing down a typical fjord inset into the alpine terrain of eastern Baffin Island, with erosive ice limited to the fjord proper, and non-erosive cold-based ice mantling the adjacent uplands, where the potential is high for lakes that record multiple interglacial sediment records.

clastic units between interglacial gyttja are commonly stiff and sometimes stony. Most lakes were cored in spring (May) using lake ice as a coring platform; a few lakes were cored in summer from a floating platform. Cores were returned intact to home institutions where they were split longitudinally and described before sampling. Geotek scanning (e.g. LacCore, U. Minnesota) was undertaken for most cores.

Terminology

We use the term ‘interglacial’ (*sensu lato*) to describe intervals of stratified, organic-rich lacustrine sediment, similar in character to Holocene gyttja. ‘Interglacial’ sediments were deposited when an ice sheet, or its meltwater, were not present in the lake’s catchment and the lake was open in summer. We use the term ‘deglacial’ to describe dominantly minerogenic lake sediment deposited rapidly by meltwater when a glacier margin was in the catchment, releasing significant volumes of surface run-off and delivering eroded catchment soils and/or glacially eroded sediment to the lake basin. We use the term ‘Last Interglacial’ (LIG) for sediment we consider to be a temporal equivalent of MIS 5e with support from luminescence dates and pollen data. We use the marine-isotope-derived time-scale to suggest the ages of other units.

With the objective of synthesising observations and data spanning several decades and many lakes, we utilise a stratigraphic nomenclature that facilitates between-lake comparisons and supplants the various numbering schemes employed in previous publications. The new numbering system is keyed to the longest and most stratigraphically complete site to date, Lake CF8 (Axford *et al.* 2009b). Most other sites do not contain all the units described below. However, this slight inconvenience is outweighed by the utility these units represent in terms of correlation tools across the region of interest. The primary units (Fig. 6) in chronological order are:

Unit 1ox: Gyttja, ‘oxidised’ sediment.
Unit 1ao: Gyttja ‘anoxic organic’ sediment.
Unit 2min: ‘Minerogenic’ sediment, although in several lakes this includes organic material, commonly producing discordant palaeoclimate proxies and highly variable and inconsistent ^{14}C ages.
Unit 2gl: Diamict, ‘glacial’ in origin.
Unit 3co: ‘Compact organic’ horizon, stratified, stone-free, bryophyte-rich; found only in the four adjacent lakes near the Clyde River.
Unit 4min: ‘Minerogenic’ stratified deglacial sediment, found only in the four adjacent lakes near Clyde River between Units 5 and 3.
Unit 5co: ‘Compact organic’ sediment (gyttja), often with abundant bryophyte remains. Although the thickness of Unit 5 is often approximately half that of Unit 1, the mass is similar to the mass of Unit 1 in the same lake.
Unit 6min: ‘Minerogenic’ sediment, deglacial in origin.
Unit 6gl: Diamict, ‘glacial’ in origin.
Unit 7co: ‘Compact organic’ sediment (gyttja).

Accelerator mass spectrometry radiocarbon dating

We date plant macrofossils, usually aquatic moss, and in some instances humic acid extracts. Most samples were graphitised at the Laboratory for Accelerator Mass Spectrometry (AMS) Radiocarbon Preparation and Research (NSRL), INSTAAR, University of Colorado, Boulder, and measured at the W.M. Keck Carbon Cycle Accelerator Mass Spectrometer at the University of California Irvine; a few were measured at the National Ocean Sciences Accelerator Mass Spectrometry at Woods Hole Oceanographic Institution, and some samples were processed and measured at the University of Arizona. We consider plant macrofossil ^{14}C ages to be the most reliable constraint on the ages of Holocene gyttja, and all ^{14}C ages ≥40 ka to be limiting ages (see Wolfe *et al.* 2004 for summary of ^{14}C lake dating). All ^{14}C ages from earlier work have been recalibrated using Intcal20 and given as ‘ka’; ^{14}C ages beyond the calibration range are reported as >55 ka, or their reported age when >55 ka (Supplemental Table S1).

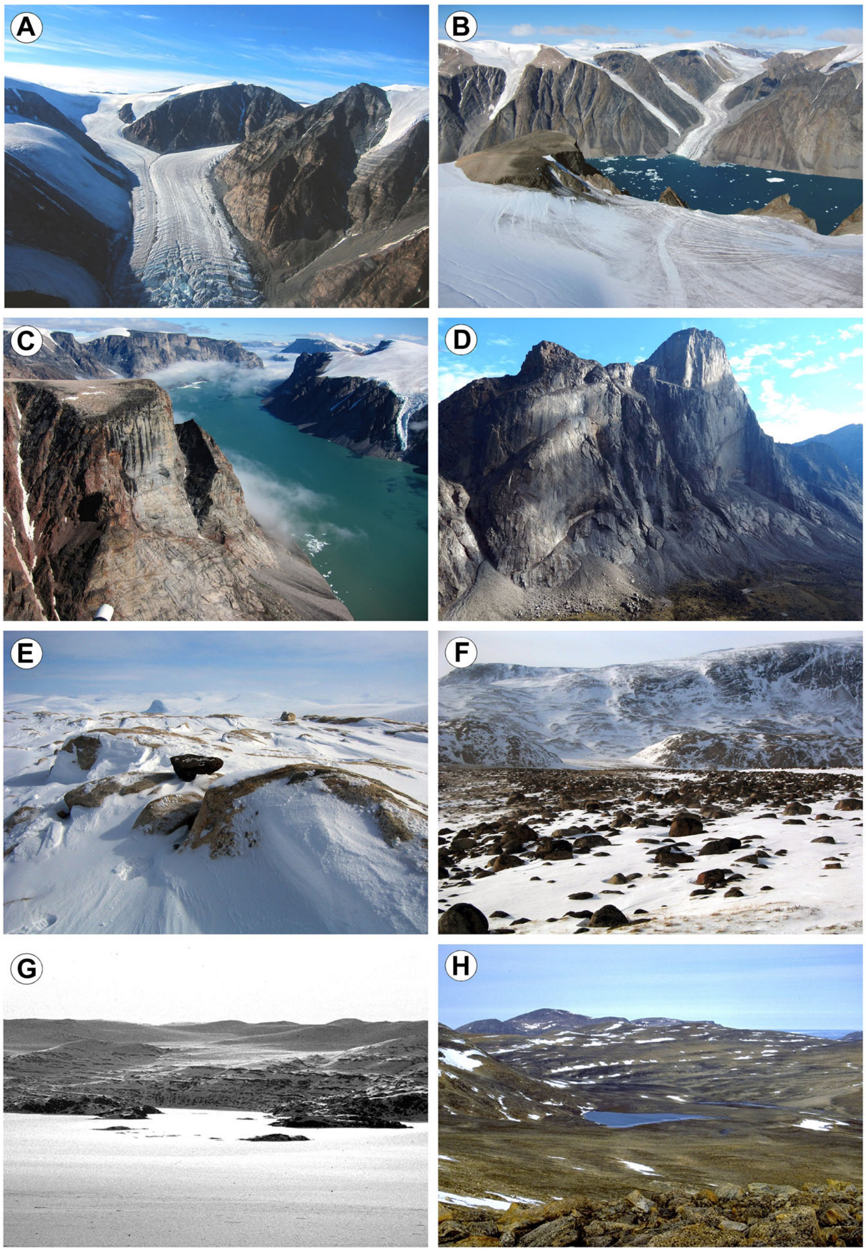

Figure 4. Imagery representative of Baffin Island landscapes. A) Unnamed outlet glacier draining a local ice cap, northeast Baffin Island. B) Local outlet glaciers reaching sea level, northeast Baffin Island. C) North Arm, northeast Baffin Island. D) Mount Thor (1675 m elevation), Pangnirtung Pass, Baffin Island. E) Interior plateau of Baffin Island. F) Moraine-dammed lake G) Lateral moraines marking an outlet glacier of the Laurentide Ice Sheet on the eastern coast of Baffin Island; such moraines often dam lakes. H) Fog Lake, Baffin Island. All photos by J. Briner or G. Miller. [Color figure can be viewed at wileyonlinelibrary.com]

Luminescence dating

An alternative for age control of lake sediment beyond the range of radiocarbon dating is provided by luminescence dating. The luminescence signal is dependent on the stability of electrons in clastic grains when disturbed by the flux of radiation emitted from a sphere of ~30 cm diameter surrounding the sample, which limits the number of samples suitable for luminescence dating in sediment cores. Luminescence also requires sufficient solar exposure during sediment transport to reset any previously acquired luminescent signal. We test these requirements for interglacial sediment by comparing the luminescence and radiocarbon ages of Holocene sediment with similar physical characteristics in the same sediment core. If the luminescence and radiocarbon Holocene ages are in close agreement, we assume that in similar depositional environments deeper in the same core, adequate zeroing of the luminescence signal occurred. We tried thermoluminescence (TL), infrared-stimulated luminescence (IRSL), red-stimulated luminescence (RSL) and optically stimulated luminescence (OSL) on both sand- and silt-sized sediment and on both quartz and feldspar fractions, with the most encouraging results from OSL on feldspars in the silt fraction (Wolfe *et al.* 2004). Luminescence dating was used to constrain the ages of Unit 5co sediment from RL, FOG, BRO and CF8 lakes. One-sigma uncertainties in our luminescence ages are >±10%, which hinders secure placement in the global marine isotope chronology.

Environmental proxies (Fig. 7)

We utilise a range of environmental proxies that are described in detail in the original papers for lakes discussed below. Biotic proxies include pollen (e.g. Fréchette *et al.* 2006), midge taxonomy (e.g. Francis *et al.* 2006; Axford *et al.* 2011, McFarlin *et al.* 2018), diatoms (e.g. Wolfe, 1994), biogenic silica (BSi) determined by Fourier transform infrared spectroscopy (Meyer-Jacob *et al.* 2014) as a measure of diatom productivity, and sedaDNA as a reliable measure of vascular plants living in close proximity to the lake (Crump *et al.* 2021). Other proxies include bulk geochemistry (C and N concentrations and their stable isotopic composition), water content, wet bulk density and volume MS, which across the study region reliably differentiates dominantly minerogenic sediment, characteristic of episodes when glacier meltwater dominates sediment delivery, from interglacial periods, when biogenic production dominates over the minerogenic component.

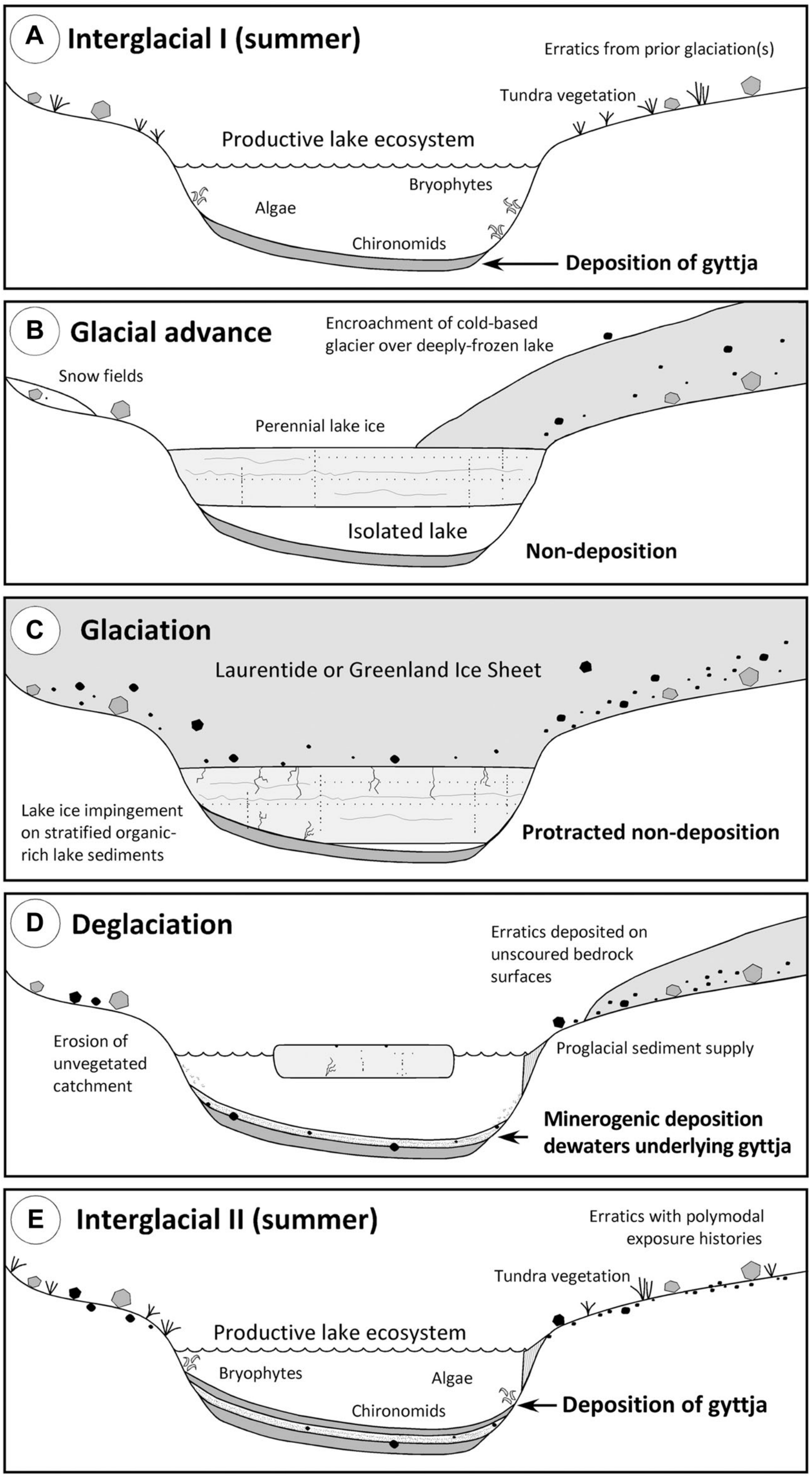

Figure 5. Conceptual model of lake sedimentation through an interglacial–glacial–interglacial cycle. A) Interglacial summer, productive lake and stable catchment. B) Summers cool as climate transitions to glacial mode; lake remains ice-covered through summer before cold-based portion ice-sheet advances across the lake, preventing sediment from being deposited in the lake; preglacial lake sediment is protected from erosion. C) Lake is covered by a thick, cold-based sector of the ice sheet; lake cannot totally freeze due to the inability to dissipate latent heat released on freezing. D) During deglaciation, summers are warm enough that the lake ice melts as soon as the ice sheet leaves the lake. Sediment is dominantly minerogenic, eroded from the catchment by meltwater, and transported to the lake as long as the ice sheet remains within the lake's catchment. The weight of the minerogenic sediment slowly dewaters the underlying gyttja, compacting the sediment. E) Once the ice sheet leaves the catchment, vegetation quickly stabilises hillslopes, and gyttja sedimentation dominates.

Stratified interglacial sediment from lakes along eastern Baffin Island and northwest Greenland

Lake sediment records have distinct chronological advantages over isolated organic-bearing deposits, in that the time domain of sedimentation is in a distinct chronological order, and the sedimentary layers record deposition whenever the lake is at least seasonally ice-free. Consequently, lakes in glaciated terrain that contain pre-Holocene interglacial sediment offer the potential to test hypotheses regarding local ice-sheet recession by the ages and frequency of interglacial units preserved in their sedimentary records. With a wide range of biotic, physical and geochemical climate proxies preserved in interglacial units, comparisons of summer temperatures and moisture balance in previous interglacials with those of the Holocene are possible. For these reasons lake sediment cores have been targeted by the palaeoclimate community as ideal archives to record climate evolution throughout the past.

The first stratified interglacial lacustrine sediments beyond the range of radiocarbon dating and interpreted to be of Last Interglacial age were recovered from Robinson and Amarok lakes in 1991 (Wolfe, 1994; Miller *et al.* 1999). In subsequent field campaigns, stratified interglacial sediments below Holocene gyttja were recovered from 10 other lakes on Baffin Island, and one in northwest Greenland (Fig. 2). Below, we

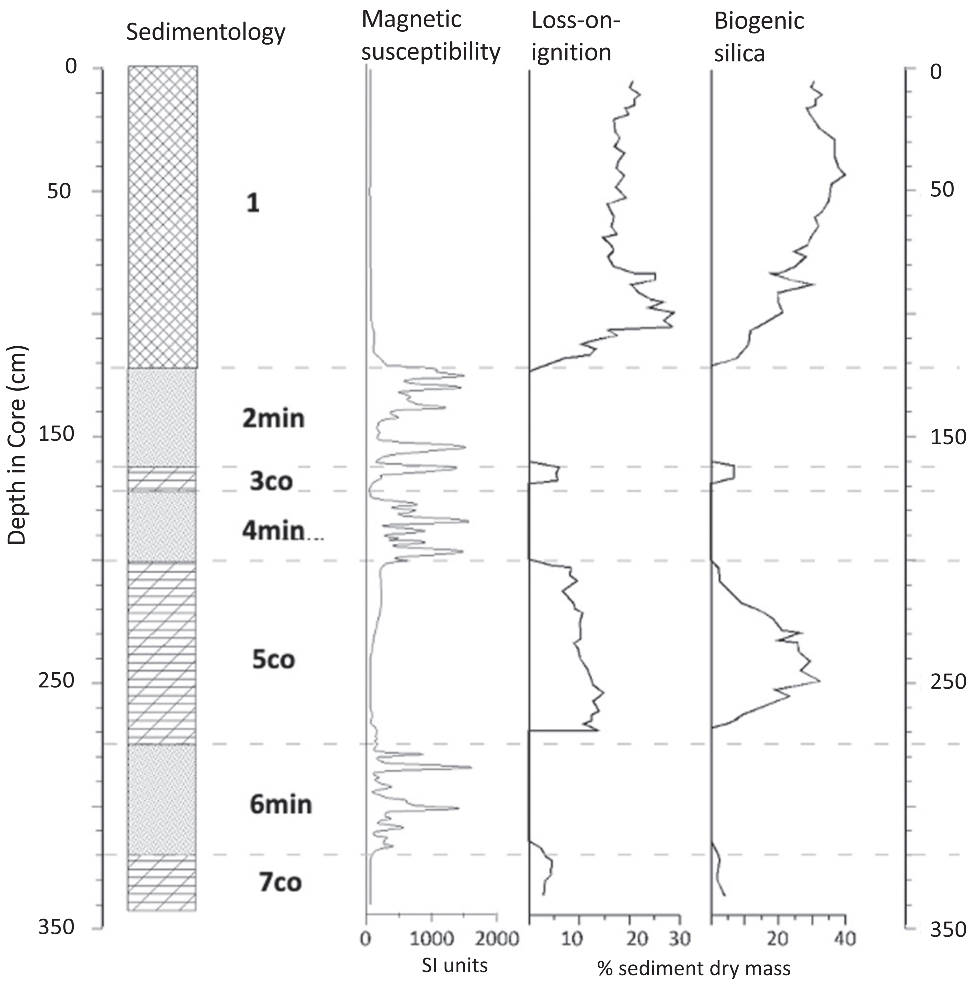

Figure 6. A conceptual sediment core from a lake that has experienced four discrete interglaciations following the sedimentation model described in Fig. 5; Gyttja units (hatched), increasingly dewatered with depth; minerogenic units (stippled). Magnetic susceptibility tracks the relative proportion of mineral matter; loss on ignition is proportional to organic matter content, and biogenic silica tracks diatom abundance.

summarise the setting, stratigraphy, geochronology and climate inferences derived from those 13 lakes in a south-to-north transect (Table 1).

Robinson Lake, Brevoort Island (RL) (Miller et al. 1999)

Robinson Lake (Fig. 8) is a small (17 ha) lake constrained by a sediment dam at the drainage divide 160 m asl on Brevoort Island, southeast Baffin Island. Brevoort Island was fully inundated by the LIS at the LGM (Dyke *et al.* 2002). Sediment cores were obtained through lake ice in May 1991 and 1993. The 1991 cores 91-RL3 and 91-RL4, in a water depth of 10 m, recovered Holocene gyttja, beneath which was ~20 cm of diamict containing stones similar in diameter to the core barrel, with a sharp basal contact to stratified lacustrine sediment with twice the density of Holocene gyttja, presumably due to dewatering from the weight of the overlying diamict. The 1993 coring campaign focused on the 14 m central deep. Six sediment cores recovered sub-till stratified lacustrine sediment (Unit 5co; Fig. 9); core 93-RL10 also recovered a second diamict below 40 cm of sub-till interglacial sediment. Freshwater diatoms are common in all levels of stratified sediment, confirming they are lacustrine.

Seven AMS ^{14}C dates on moss macrofossils in Unit 5 from two different cores are all >40 ka, indicating that the interglacial is beyond the range of ^{14}C dating. Thermoluminescence, IRSL and RSL were measured in interglacial sediment from core 93-RL4. Three samples were early Holocene sediment (80–100 cm depth) and two were from sub-till interglacial sediment representing peak warmth based on pollen (190–196 cm depth). Luminescence ages of the early Holocene sediment averaged 7 ± 3 ka and from the pre-Holocene interglacial sediment ranged from 96 ± 10 ka to 66 ± 7 ka, with an average age of 85 ± 10 ka (Miller *et al.* 1999). These results confirm a MIS 5 age, but uncertainties in calculating the dose rate from a sediment core, and their wide age ranges leave the absolute age within the MIS 5 time window uncertain.

Pollen and diatom analyses were undertaken from the Holocene of 91-RL4, and Unit 5 of 91-RL4, 93-RL3 and 93-RL10 (Fig. 10). In 91-RL4 Holocene sediment *Alnus* pollen begins to rise ~7 ka, peaks at ~6 ka, declining thereafter. The diamict separating Holocene from older interglacial sediment is barren of pollen, but pollen concentrations in Unit 5 of 91-RL4 are similar to those of the early Holocene, and pollen assemblages in Unit 5 from both 91-RL4 and 93-RL3 are dominated by *Alnus* and *Betula*, with *Alnus* pollen exceeding 40% of the pollen sum in several levels.

Evidence of summer warmth during the deposition of Unit 5 in excess of any time during the Holocene is based on *Betula* pollen, which accounts for 50 to 60% of the endogenous pollen sum, in contrast to no more than ~20% throughout Holocene sediment. Such a dominance requires *Betula* to be growing near the lake during deposition of Unit 5. The nearest stands of *Betula* at present are ~200 km to the west at interior sites where a more continental climate currently provides 2.5°C greater summer

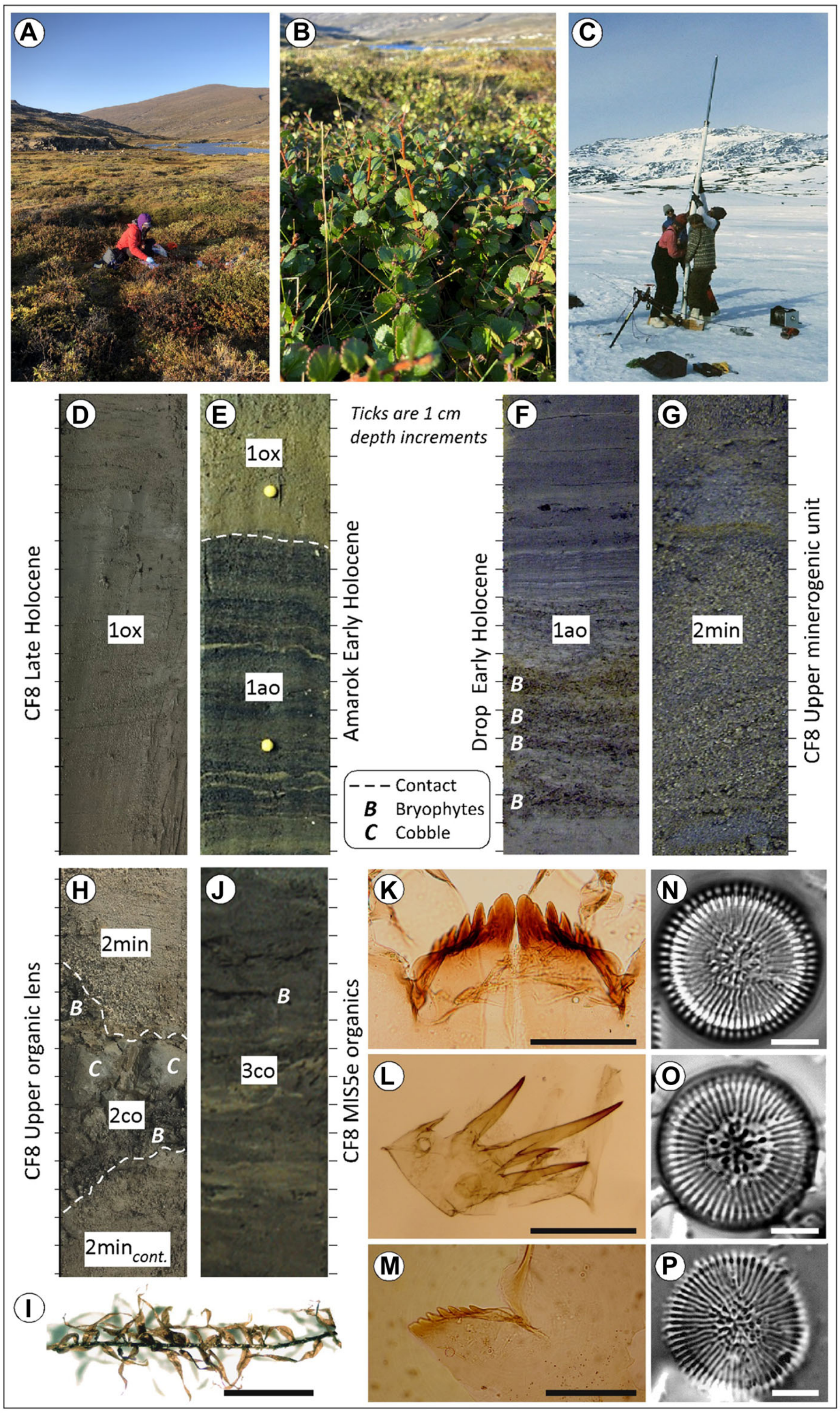

Figure 7. Biological examples and lacustrine facies. A) Shrub birch thicket, head Padle Fjord (near Fog Lake). B) *Betula nana* (shrub birch). C) Coring Lake CF8. D) Holocene gyttja from Lake CF8. E) Contact between oxic and anoxic Holocene gyttja in Lake AKL. F) Contact between oxic and anoxic Holocene gyttja in Lake DRP. G) Contact between Holocene gyttja (above) and minerogenic MIS 2 deglacial sediment in Lake CF8. H) Mossy interglacial unit (moss (image I) ^{14}C >45 ka) underlain and overlain by deglacial sand at Lake CF8. This layer probably represents brief deglaciation in late MIS 5. J) Last Interglacial gyttja in lake CF8. K, L, M) Chironomid head capsules from LIG mud in Lake CF8. N, O, P) Diatoms from LIG mud in Lake CF8. [Color figure can be viewed at wileyonlinelibrary.com]

temperatures than found in maritime regions where RL is situated (Iqaluit mean temperature for June–August (JJA) 6.4°C vs Brevoort Island JJA 4.0°C.)

The primary explanation for preservation of ancient sediment at RL is its setting relative to the flow of Laurentide ice based on striations throughout the region. The lake occupies a depression in a valley trending northeast–southwest across Brevoort Island. Striations in the vicinity of the lake parallel the strike of the valley, but are at right angles to primary Laurentide ice flow in the region, which is constrained by the channel separating Brevoort Island from mainland Baffin Island oriented to the south-southeast–north-northwest. Consequently, flow across RL is driven only by the shallow surface gradient on the LIS there, suggesting relatively low velocities and limited erosion, although striae are preserved.

Amarok Lake (AKL), Cumberland Peninsula (Wolfe, 1994; Fréchette et al. 2006)

Amarok Lake is a small (4 ha) lake, 850 m asl near the drainage divide in uplands lacking diagnostic glacial erosional features and surrounded by highly weathered felsenmeer. Stratified pre-Holocene interglacial sediment was recovered from AKL in 1991 and 1998. A 205 cm long sediment core recovered through lake ice in 1998 contained 120 cm of Holocene gyttja, non-conformably overlying almost a metre of compact,

Table 1. Lake name, location, and number of superposed 'interglacial' units recovered from sediment cores

Lake	Informal name	Latitude	Longitude	# of interglacials
RL	Robinson Lake	63.3989	−64.2600	2
AKL	Amarok Lake	66.2917	−65.7729	2
BIR	Akvaqiak Lake	66.7993	−63.9694	1
FOG	Fog Lake	67.1824	−63.2503	2
BRO	Brother of Fog Lake	67.1925	−63.1368	3
SAD	Saddle Lake	67.0662	−62.7036	2
GNR	Gnarly Lake	67.2172	−63.0282	2
CAN	Canso Lake	67.2059	−63.5688	2
AMA	Amakuttalik Lake	67.8064	−64.5673	1
CF8	Lake CF8	70.5580	−68.9502	4
ATA	Lake Attata	70.5642	−68.9740	4
SPT	Spot Lake	70.5613	−68.9622	3
DRP	Drop Lake	70.5319	−68.9231	3
AFR	Africa Lake	72.4193	−77.4460	2
WLL	Wax Lips Lake	76.8516	−66.9586	2

stratified, silty gyttja (Unit 5). Aquatic bryophytes from the top and middle portions of Unit 5 are 46.0 ka and 47.9 ka, respectively (Fréchette *et al.* 2006).

Pollen was analysed from 25 evenly spaced levels through the Holocene section and 18 levels through Unit 5 (Fig. 11). Pollen concentrations in Unit 5 average ~100 000 grains cm^{-3}, compared with <1000 grains cm^{-3} for most of the Holocene. Dewatering of Unit 5 sediment may account for a ~50% increase in pollen concentrations based on sediment volume, but does not alter the conclusion that pollen concentrations, which equate to biological productivity, were dramatically higher during Unit 5 time, than at any time during the Holocene.

Betula dominates the pollen counts through Unit 5, accounting for 40 to 50% of all pollen grains, whereas *Betula* pollen accounts for 10 to 20% throughout the Holocene. *Betula* currently grows below 100 m asl 100 km southwest of AKL, but *Betula* must have been more abundant and growing at higher elevations during deposition of Unit 5, given the higher *Betula* pollen concentrations and percentages. The lower abundance of herb pollen grains coupled with high concentrations of both *Betula* and *Alnus* pollen in Unit 5 compared with Unit 1 suggests that not only was *Betula* growing nearby, but plausibly *Alnus* was growing on Baffin Island during Unit 5 time.

Amarok Lake has high preservation potential due to its high elevation in a landscape devoid of glacial erosional features. The lake is situated in a triangular massif bordered by wide valleys and adjacent to the 1200 m deep Cumberland Sound that efficiently channelled Laurentide ice into Baffin Bay.

Merchants Bay lakes, northeast Cumberland Peninsula

We recovered pre-Holocene stratified lacustrine gyttja from five lakes in the Merchants Bay region (Fig. 12), in most cases separated from Holocene gyttja by minerogenic lacustrine sediment.

Fog Lake (FOG) (Steig *et al.* 1998; Wolfe *et al.* 2000; Joynt and Wolfe, 2001; Francis *et al.* 2006; Fréchette *et al.* 2006, 2008a).

Stratified pre-Holocene interglacial sediment was recovered from FOG (Fig. 4), a small (6 ha) lake, 460 m asl, in 10 m water depth from the lake ice with a sledge-mounted percussion coring system in 1996 and 1998. Core 96FOG-05 (Fig. 13B) captured 137 cm of sediment: 51 cm of Holocene gyttja (Unit 1), over 29 cm of mineral-rich silts (Unit 2), underlain by 30 cm of compact gyttja (Unit 5co) which overlies 10 cm of laminated clay-rich silts (Unit 5min), and 20 cm of stony diamict (Unit 6gl) with clasts with up to 11 cm long axes.

Wolfe *et al.* (2000) report 16 ^{14}C dates through 96FOG-05. Moss from the top of Unit 2 has an age of 9.1 ka, constraining Unit 1 to the last 9.1 kyr. Minerogenic Unit 2 (3% C vs 10 to 15% C in the overlying gyttja) is considered deglacial sediment. Nine radiocarbon dates through Unit 2 illustrate the complexity in constraining ages of some deglacial units. Mixed plant fragments from 80 cm depth at the base of Unit 2 have a ^{14}C age of 36.8 ka, but aquatic moss 7 cm higher have a ^{14}C age of 9.5 ka. In contrast, humic acids extracted from 75 and 71 cm depth are 19.0 and 19.4 ka, respectively. Underlying stratified compact gyttja (Unit 5) has non-finite ^{14}C ages on both aquatic moss (>55 ka), and humic acid extracts (>47 ka) from the base of the unit (110 cm depth), but finite humic acid dates of 41.1 ka and 39.9 ka higher in the unit. Interpreting these conflicting ages from Unit 2 is discussed below (see 'Ages of units').

96FOG-04, which captured the three youngest units and is correlated with 96FOG-05 on MS (Fig. 13C), was dedicated to luminescence dating. Two different luminescent procedures were used to better constrain the age of Unit 5. Thermoluminescence and IRSL ages on two levels of Holocene sediment are similar to their ^{14}C ages, confirming adequate zeroing of any previously acquired luminescence signal. Two IRSL ages from ~113 cm depth in Unit 5 gave ages of ~95 ka, while from ~125 cm depth two TL dates averaged ~86 ka, and two IRSL dates averaged 95 ka. These results confirm that Unit 5 dates from early in MIS 5 (Wolfe *et al.* 2000).

Pollen was enumerated from 71 samples spaced relatively evenly through 96FOG-05 (Fig. 13D). Holocene pollen is similar to other Holocene pollen records from Baffin Island (Miller *et al.*, 2005), but the high pollen concentrations in minerogenic Unit 2 is unusual for deglacial sediment (see 'Ages of units'). Pollen concentrations are nearly an order of magnitude higher in Unit 5co than in Holocene (Unit 1) sediment, with *Betula* and *Alnus* dominating the pollen counts. Pollen is also higher in Unit 5min and the basal diamicton (Unit 6) than in the Holocene. *Betula* pollen decreases steadily as a percentage throughout Unit 2, whereas pteridophyte spores (mostly *Lycopodium*) are consistently ~20% of the pollen and spore total, suggesting less favourable conditions for vascular plants. Both pollen concentrations and *Betula* pollen percentages decrease abruptly at the Unit 2/1 transition. The dramatically higher pollen concentrations in Unit 5co relative to Unit 1, and the dominance of *Betula* and *Alnus* pollen in Unit 5co, indicate warmer and likely longer summers during deposition of Unit 5co. Additional support for warmer summers during the deposition of Unit 5co than the Holocene is provided by the evolution of *Betula* pollen grain diameters through 96FOG-04 (Fig. 14). Large-diameter *Betula* pollen originates in more temperate ecosystems than those producing smaller grains. The large grain diameters found in Unit 5co *Betula* pollen relative to Unit 1 grains require a different plant source and is consistent with other data indicative of a consistently more temperate climate through Unit 5co than at any time during the Holocene. Inferred July air temperatures during Unit 5co derived from the pollen assemblages average about 8–10°C, well above the July air temperatures inferred from Holocene pollen of 6–7°C (Fréchette *et al.* 2008a).

Chironomid head capsules have been enumerated from Units 1–5 in 96Fog-05 (Fig. 13E; Francis *et al.* 2006). Head capsules are present in all four units, but concentrations are highest in Units 1 and 5co. Midge-inferred air and water

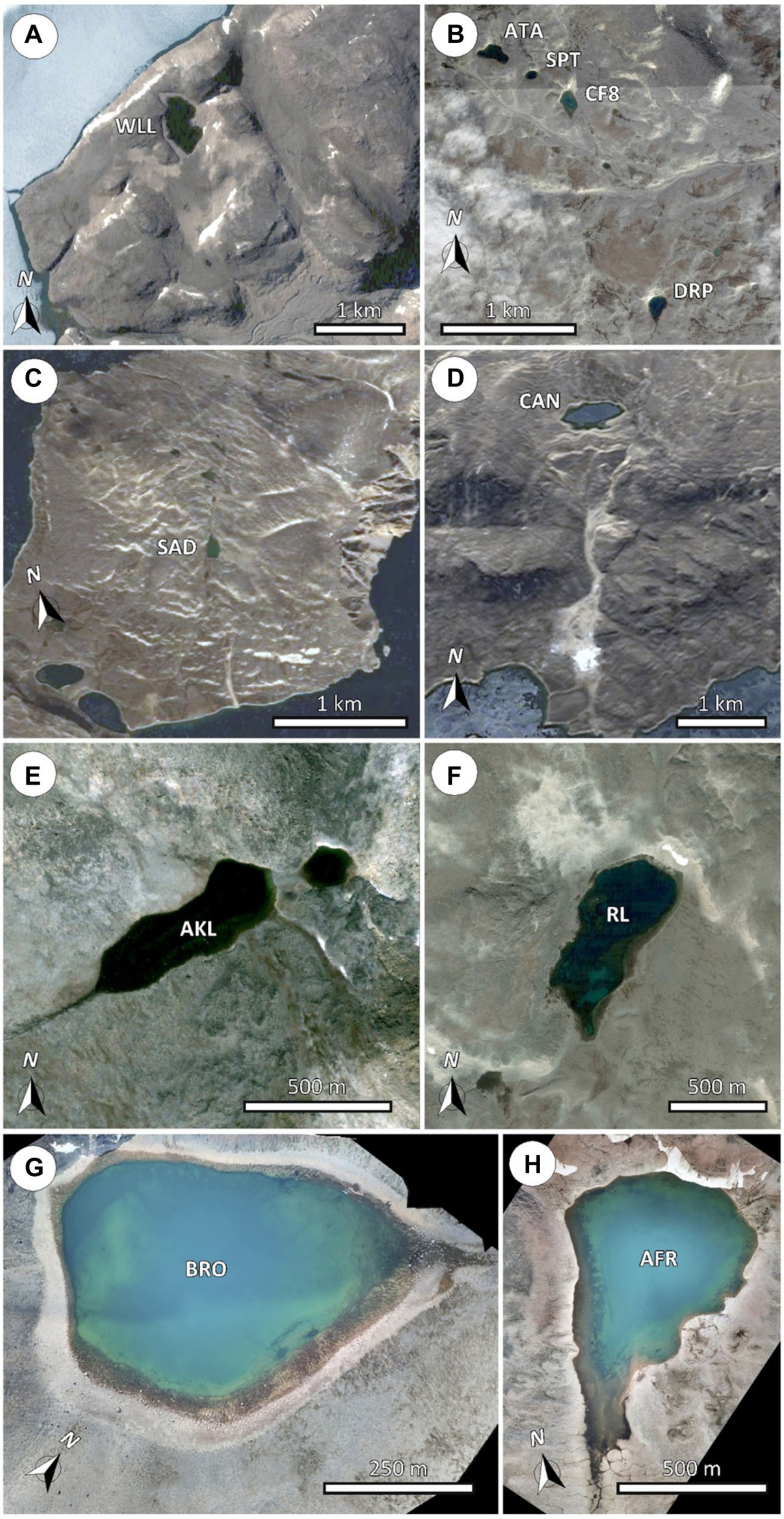

Figure 8. Images of eleven of the lakes discussed in the text. Images A–F are from Google Earth; images G and H are from drones (J. Raberg).

temperatures are estimated using an inference model. Peak summer water temperatures are predicted to be between 9 and 12°C, compared with 5°C at present; mean July air temperatures were 5–10°C higher during peak warmth of Unit 5 relative to pre-industrial times (Francis *et al.* 2006). The dominance of *Oliveridia* in Unit 2 indicates cold temperatures, low organic matter and high minerogenic sedimentation. Summer water temperatures are typically higher than summer air temperatures (Livingstone *et al.* 1999).

FOG is a moraine-dammed lake situated on a narrow bench ~50 m above the valley floor, where glacial erosion is less likely.

Brother of Fog Lake (BRO) (Steig et al. 1998; Miller et al. 2002; Francis et al. 2006)

Superposed stratified interglacial units were recovered in a series of cores from Brother of Fog Lake (BRO) through lake ice in 1998 and 2018. Field studies in summer 2019 revealed that

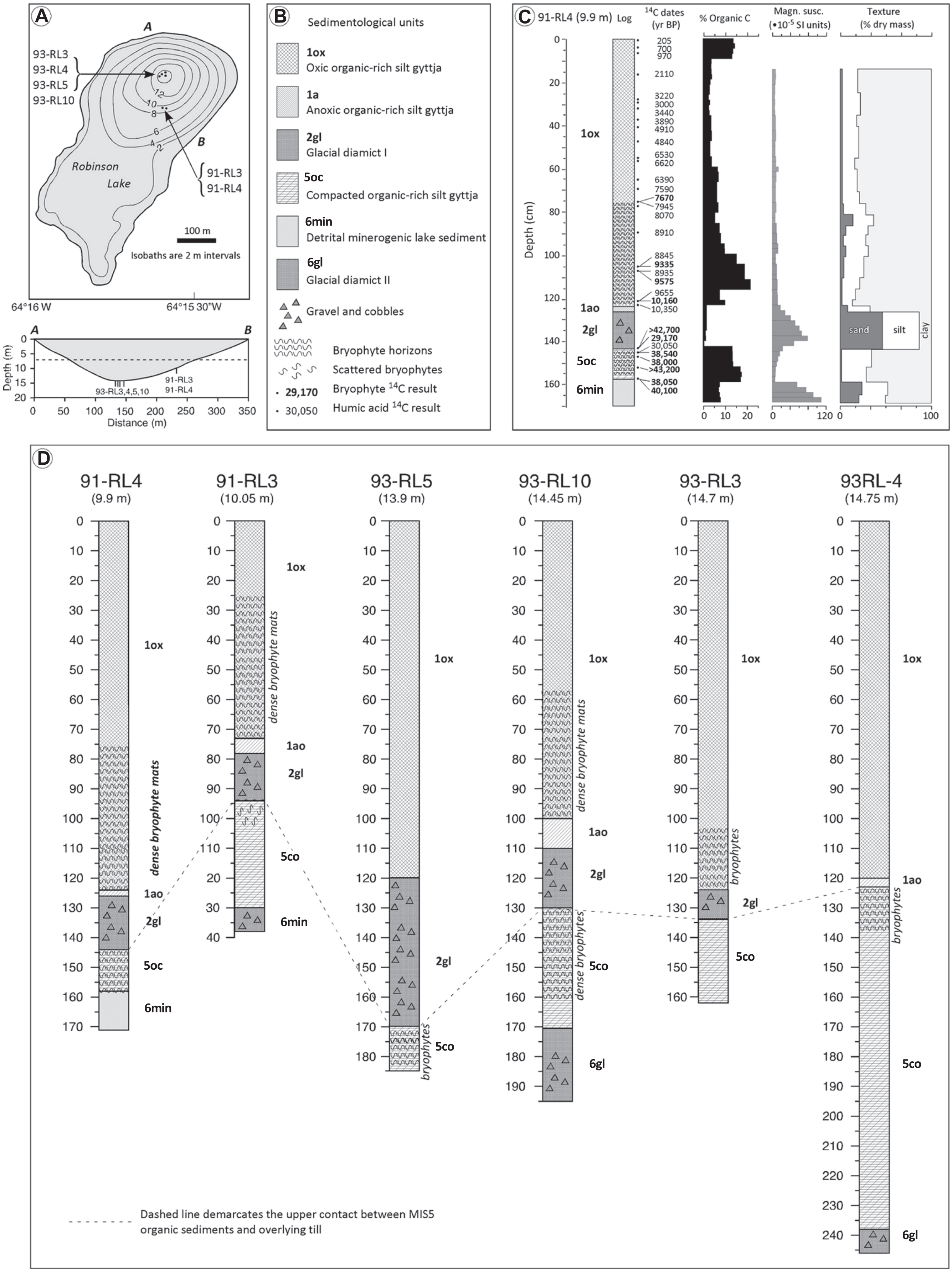

Figure 9. Robinson Lake. A) Bathymetric and cross-section maps showing the locations of cores taken in 1991 and 1993 that are discussed in the text. B and C) Sediment core 91-RL4 showing primary sedimentary units, conventional ^{14}C dates on moss and humic acids, % organic carbon, magnetic susceptibility, and grain size. D) Stratigraphic logs for Robinson Lake sediment cores recovered in 1991 and 1993 and correlations between cores. Modified from Miller *et al.* 1999).

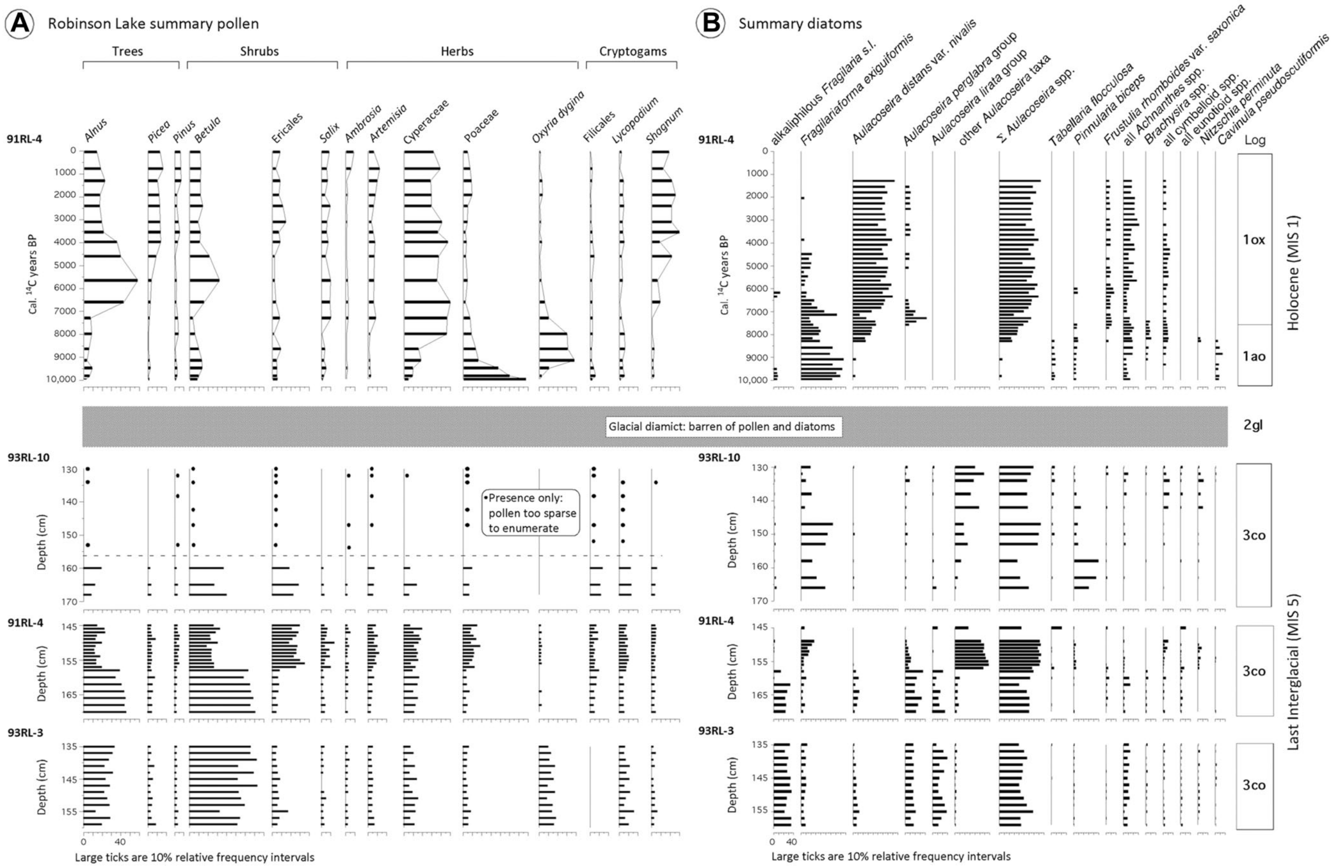

Figure 10. Down-core summaries of pollen and diatom taxa composited from three different Robinson Lake cores placed on calibrated ages for the Holocene, and depth scales for the older units (modified from Miller *et al.* 1999). The peak in *Alnus* and *Betula* ~6 ka is common to many Holocene pollen records from Baffin Island, mirroring peak *Alnus* pollen in northern Labrador/Quebec cores that was transported to Baffin Island by southerly winds.

the lake level had been raised by a sediment dam deposited during MIS 2 deglaciation delivered via a 3 km long meltwater channel draining a Laurentide outlet glacier flowing into Merchants Bay. The dam raised the lake level from a few metres to ~16 m water depth.

Sediment cores 98BRO-04 and 98BRO-05 (Fig. 15) together recovered 240 cm of sediment. A single drive with an aluminium core pipe in 2018 (18BRO-25) recovered 220 cm of sediment, with a similar stratigraphy. Five ^{14}C dates are available from each collection. The 1998 cores revealed a complex Unit 5, consisting of gyttja with variable minerogenic constituents. A ^{14}C date on aquatic moss from the top Unit 5 in the 1998 core is >60 ka and >50 ka in the 2018 core. Unit 5 is overlain by 70 cm of unconsolidated stony diamict (Unit 2min). Three ^{14}C dates on humic acids through Unit 2 in the 1998 core range from 33 to 38 ka (Francis *et al.* 2006), whereas two ^{14}C dates on moss from Unit 2 in the 2018 core are 32 ka and 33 ka. The upper 60 cm is Holocene sediment, reduced black gyttja with siderite laminae (Unit 1ao) overlain by 35 cm of olive gyttja (Unit 1ox). A ^{14}C age on aquatic moss near the base of Unit 1ao in 18BRO-25 is 10.3 ka.

Two levels in Unit 5 (181 cm and 145 cm depth) and two in Unit 2 (118 cm and 79 cm depth) were dated by luminescence. IRSL ages from within Unit 5 display resistance of luminescence to solar resetting, indicating a population of charges stored in 'deep' thermally stable traps that were not fully solar reset during sediment transport, resulting in maximum limiting ages, indicating Unit 5 sediment is no older than 125 ka. Luminescence in the two samples from Unit 2 were saturated, indicating little solar resetting of an earlier acquired luminescence signal, consistent with rapid deposition in turbid glacier meltwater (Francis *et al.* 2006).

Unit 5 pollen (Fig. 15B) reveals an ecosystem consistent with summer temperatures above mid-20th century levels, with pollen concentrations ~30 000 grains cm^{-3}. Holocene pollen was not isolated from BRO, but at nearby FOG at about the same elevation, Holocene pollen concentrations were ~4000 grains cm^{-3}. *Betula* dominates the pollen spectra throughout Unit 5, accounting for 50 to 60% of all grains; *Alnus* accounts for another 15%. Although pollen is present throughout overlying Unit 2, pollen concentrations are 25% of the concentrations during peak warmth of Unit 5.

Chironomid head capsules (Fig. 15C) were identified from 33 levels through the composite section, including the Holocene (Francis *et al.* 2006). Head capsules were present in all samples, but were most abundant in Unit 5co where 300–700 capsules were counted per gram of sediment, compared with 100–200 in Holocene sediment. Thermophilous taxa are most abundant in Unit 5, but persist into Unit 2, although at much lower abundances, and are absent from Holocene sediment. The reconstructed peak July air temperatures based on chironomid taxa from Unit 5co is ~13.5°C, whereas the reconstructed Holocene mean July temperature is 6°C (Francis *et al.* 2006), slightly below the mean July air temperature recorded at the site in 2019 of 7.0°C.

Saddle Lake (SAD) (Steig et al. 1998; Miller et al. 2002)

Saddle Lake is a small (7 ha), shallow (3 m), sediment-dammed lake nestled in a topographic saddle 260 m asl on Padloping Island, Merchants Bay (Fig. 12), with a catchment of only 2.4 km^2. Sediment in Unit 5 had been frozen into large blocks, but the stratigraphy was preserved. SAD is the only lake to

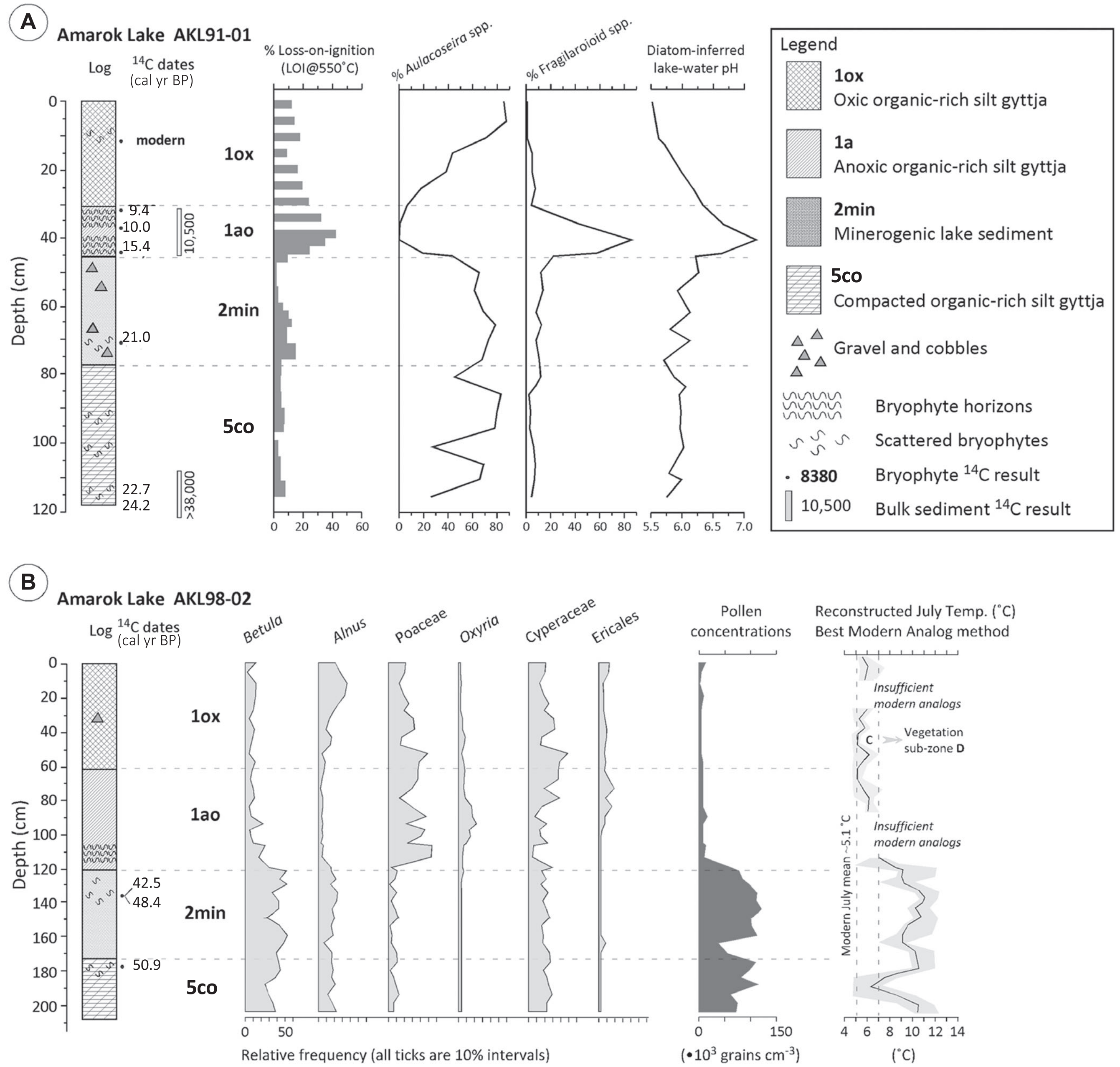

Figure 11. Logs for Amarok Lake sediment cores recovered in 1991 and 1998 (Wolfe, 1994; Miller *et al.* 2002). The radiocarbon ages are at the limit of the method The pollen-inferred temperatures suggest Unit 5co was ~5°C warmer than the Holocene.

exhibit freezing of the sediment fill, presumably due to the shallow nature of the lake; Unit 1 sediment was never frozen. A sediment core from the lake ice in 1996 (96SAD-04) recovered 235 cm of sediment, including 130 cm of Holocene gyttja; aquatic moss from the base of nearby core 96SAD-03 has a ^{14}C age of 12.9 ka. Unit 1 is underlain by 77 cm of lacustrine sediment (Unit 5co), which overlies a diamict (Unit 6; Fig. 16B). Plant macrofossils from two layers in Unit 5co are both >55 ka. Pollen was analysed from two levels in Unit 1 and two levels in Unit 5. Pollen concentrations in Unit 5co are 98 000 grains cm^{-3}, dominated by *Betula* (56%) and *Alnus* (21%), whereas the two Holocene samples have only 17 000 and 10 000 grains cm^{-3}, and *Betula* accounts for 8 and 22%, respectively, with *Alnus* only 4% in each level.

Saddle Lake was targeted as a lake with potential for a long record because it is in the centre of Merchants Bay, which has limited access to ice discharge from the LIS. The Padloping uplands are dominated by weathered bedrock that lack striations; quartz veins stand 10 cm in relief above the surrounding bedrock. A quartz vein sampled above SAD (M96-B6; 475 m asl) has a ^{26}Al/^{10}Be ratio of 4.86 ± 0.06 (Pendleton, 2018), well below the production ratio, indicating significant burial beneath an ice sheet with limited or no erosion.

Gnarly Lake (GNR) (Steig et al. 1998; Miller et al. 2002)

Gnarly Lake is elongate (700 m by 200 m) with a maximum water depth of 9 m (Fig. 12). The lake is dammed by a 12 ha ice-contact delta deposited by an LGM lateral meltwater stream of an outlet glacier in Merchants Bay that delivered sandy sediment into what was previously a shallower lake, disturbing the uppermost pre-existing sediment and leaving a higher dam following deglaciation. Sediment core 96GNR-01, recovered from the central deep in 1996, contained 275 cm of sediment (Fig. 16A). The upper

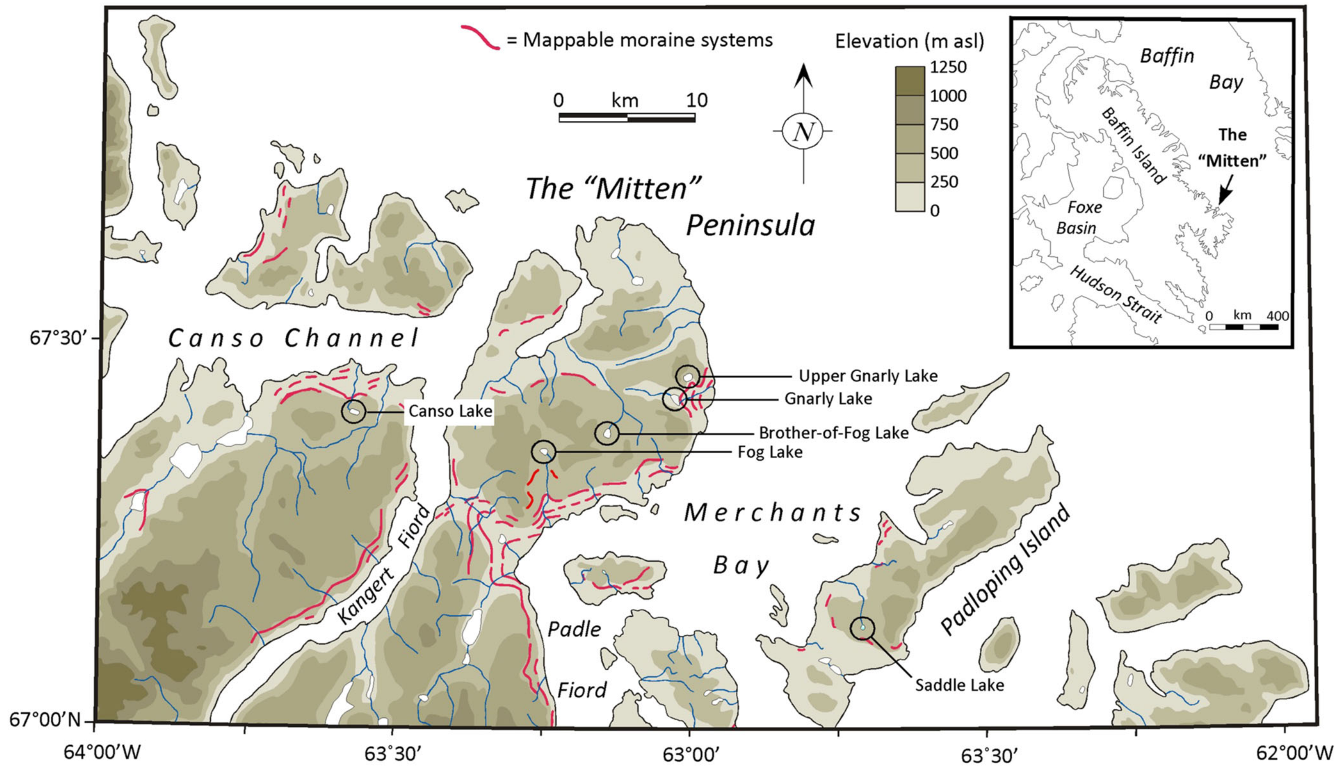

Figure 12. Map of the Merchants Bay region, Cumberland Peninsula, Baffin Island, showing the locations of lakes discussed on the text. [Color figure can be viewed at wileyonlinelibrary.com]

148 cm (Unit 1) are gyttja, with a ^{14}C age on aquatic moss at 140 cm depth of 11.7 ka. Below 148 cm a sandy unit grades downward into dense gyttja (Unit 5). Aquatic moss from 182 cm depth has a ^{14}C age of 47 ka. Pollen concentration from the early Holocene at 125 cm depth revealed 8000 grains cm^{-3} dominated by Cyperaceae (40%), with 8% *Betula* and 5% *Alnus*, whereas the pollen concentration at 220 cm depth in Unit 5 is 101 000 grains cm^{-3}, dominated by *Betula* (40%), followed by Cyperaceae (20%), although *Alnus* is only 3%.

Gnarly Lake was targeted because the dam that is responsible for the current lake level was at that time thought to have been deposited by an outlet glacier in MIS 6. However, subsequent cosmogenic exposure dating has shown that the LGM ice limit was well above Gnarly Lake (Steig *et al.* 1998). Preservation of pre-Holocene sediment in lakes around Merchants Bay is a result of both the physiographical separation of the Merchants Bay region from the rest of Baffin Island and nearby efficient routes to evacuate ice from the Laurentide and local ice caps through the 35 km-wide Merchants Bay to Baffin Bay (Fig. 12), leaving only cold-base ice on the bordering uplands. This probably explains the preservation of LIG sediment in FOG, BRO, SAD and GNR, although all four lakes are sediment-dammed.

Canso Lake (CAN) (Miller et al. 2002)

Three large fjords delivered Laurentide outlet glaciers to Canso Channel (Fig. 12) at the LGM. Canso Lake, an oblong lake of ~17 ha, 330 m asl (Fig. 12), is dammed by a 200 m-wide complex of nested lateral moraines that represent outlet glacier margins during multiple Late Quaternary glacial cycles. The crest closest to the lake is ~10 m higher than the lake, whereas the crest farthest from the lake is more than 10 m lower. Two cores, 98CAN-05 (155 cm; Fig. 16C) and 98CAN-06 (195 cm) were recovered from the wide central deep between 9 and 10 m. Although no biotic palaeoclimate proxies have been evaluated, loss on ignition and MS data define superposed interglacial units separated by clastic sediment. Unit 1 captured the Holocene in 80 cm of sediment, with a basal age on humic acid extracts of 13.2 ka, overlying 15 cm of dense clastic sediment (Unit 2min) presumably deposited during LGM deglaciation although no dates are available. Underlying Unit 2 are 40 cm of dense, dewatered gyttja (Unit 5co); humic acids extracted from the top of Unit 5 in 98CAN-05 have a ^{14}C age of 41.7 ka, and aquatic moss from near the base has a ^{14}C age of 45.6 ka. Aquatic moss from Unit 5co in nearby core 98CAN-06 has a ^{14}C age of >60 ka.

Clyde River lakes, northeast Baffin Island

Our teams have cored numerous lakes near the settlement of the Clyde River, northeast Baffin Island (Fig. 17A). Although most lakes record only postglacial deposition (e.g. Mode 1980), a cluster of four adjacent kettle lakes ~15 km northwest of the settlement record sedimentation during multiple deglacial and interglacial intervals.

Lake CF8 (CF8) (Briner et al. 2007; Thomas et al. 2008; Michelutti et al. 2009; Axford et al. 2009a,b; Thomas and Briner 2009; Axford et al. 2011; Wilson et al. 2012; Crump et al. 2021)

Lake CF8, a small (5 ha) kettle lake, ~10 m deep with a catchment of only 1.7 km^2, was cored in 2002, 2005, 2006, 2007, 2008, 2017 and 2019. CF8 has the most complete record of interglacial sedimentation of all 13 lakes reported here. We use the CF8 record as a type locality for interglacial (*sl*) episodes along the northeast North American Arctic, and correlate the other lake sediment records summarised here with the CF8 stratigraphy.

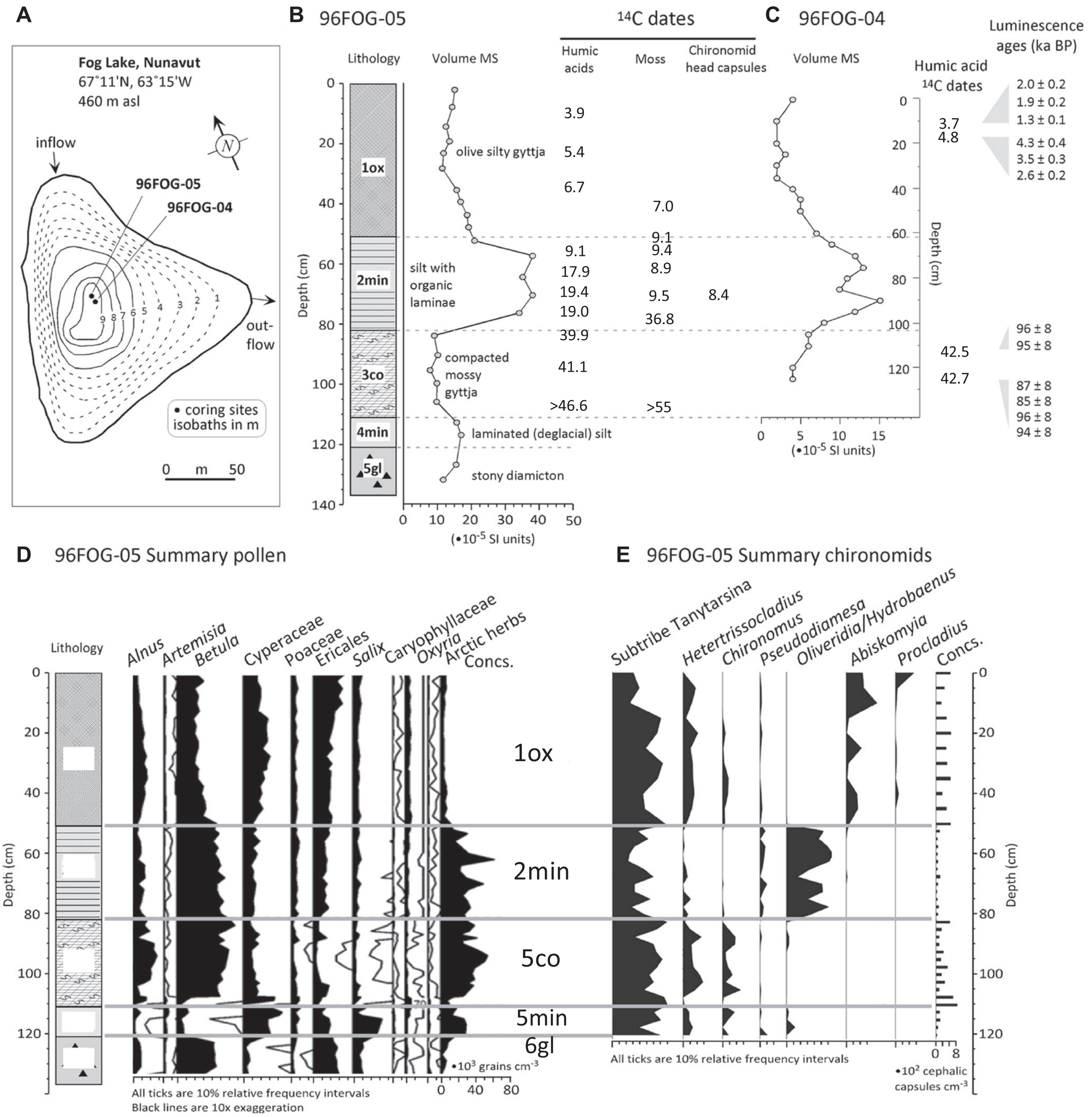

Figure 13. Fog Lake (Wolfe *et al.* 2000). A) Bathymetric map and location of 96FOG-04 and -05. B) 96FOG-05 stratigraphic log, magnetic susceptibility, and calibrated radiocarbon dates. C) 96FOG-04, with magnetic susceptibility used to correlate to 96FOG-05. Close correspondence between luminescence and radiocarbon ages in Holocene sediment lend credibility to our conclusion that luminescence dates confirm that most ^{14}C dates close to and >40 ka from lake sediment should be considered minimum ages. D) and E) summarise the palynology (Fréchette *et al.* 2006) and chironomid taxonomy (Francis *et al.* 2006) in 96FOG-05. Although Unit 2min has high levels of *Betula* pollen and high concentrations of pollen grains, giving the appearance of relative warm summers during deposition, the chironomid taxa are dominated by the cold taxon Oliveridia. We interpret Unit 2min to have been deposited in decades to centuries during local deglaciation, when Laurentide meltwater eroded Last Interglacial soils preserved in the catchment beneath cold-based ice. The moss radiocarbon date of 9.5 ka near the base of the unit marks the timing of deglaciation with humic acid dates higher in the unit, and an adjacent moss sample dated 36.8 ka, probably containing variable, but decreasing, admixtures of 'old' (^{14}C-dead) and contemporary carbon with early Holocene carbon compounds.

Briner *et al.* (2007) report three interglacial units below the Holocene, each separated by clastic sediment dominated by well-sorted sand (Fig. 17A). A ^{14}C date on aquatic moss from the base of the Holocene is 11.6 ka. The youngest pre-Holocene interglacial (Unit 3), is a thin (5 cm) packet of almost pure aquatic moss. Six ^{14}C dates on moss from Unit 3co in cores from CF8, ATA and DRP (Fig. 17) are all >40 ka (Table S1). OSL dating was used to better constrain the ages of older interglacial Units 5 and 7. OSL ages on the silt fraction isolated from Holocene sediment in CF8 gave ages consistent with macrofossil ^{14}C dates, indicating that full solar bleaching of any previously acquired luminescence signal had occurred. OSL ages on sediment from the top of Unit 5 are 97 ± 10 ka and 105 ± 10 ka, whereas basal Unit 5 sediment has an OSL age of 122 ± 12 ka (Briner *et al.* 2007). The OSL signal in silt from Unit 7 was saturated, resulting in an age of >194 ± 19 ka.

Changes in summer temperatures have been reconstructed from assemblages of midges, pollen, diatoms and ancient DNA

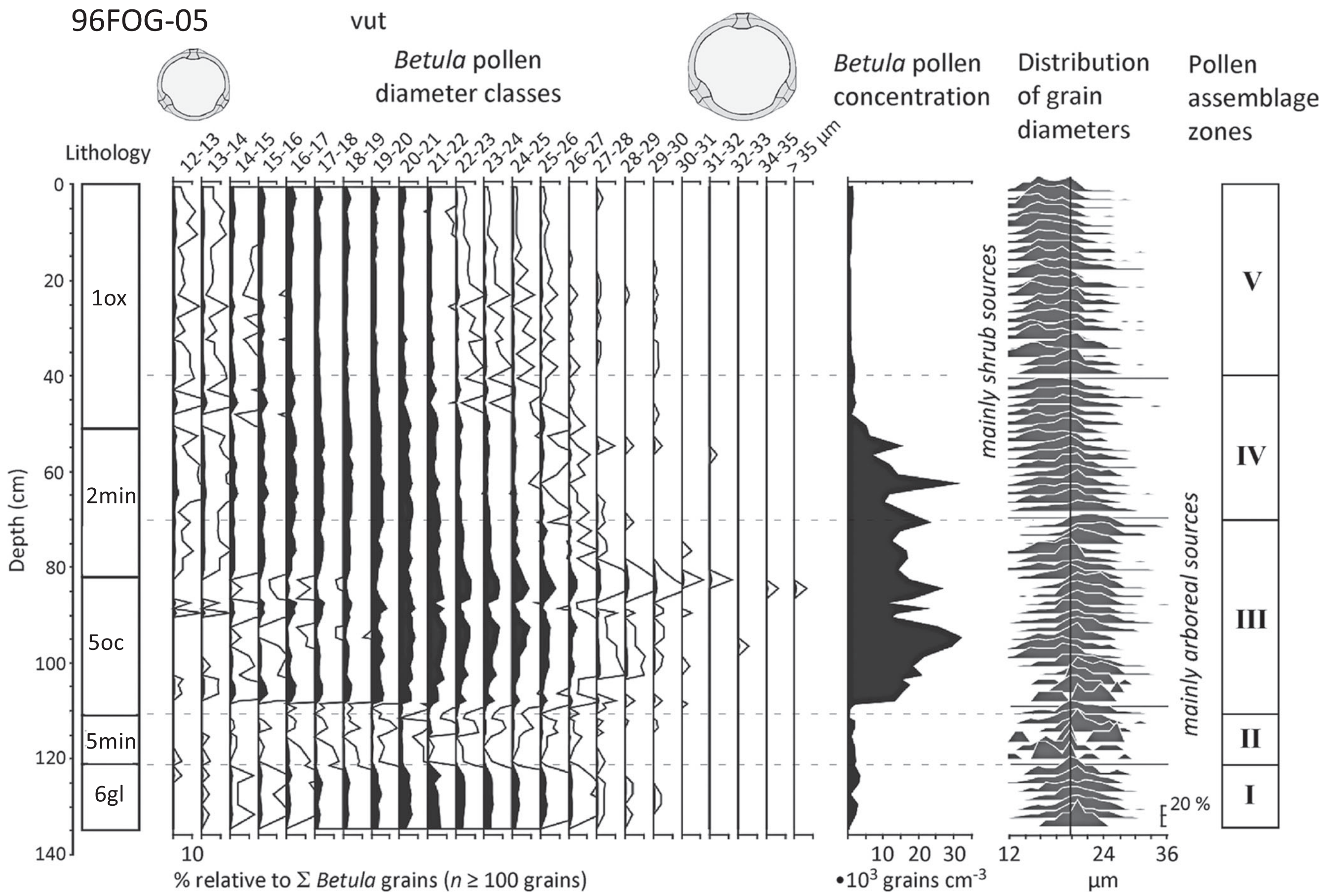

Figure 14. *Betula* pollen diameters through sediment core 96FOG-05, and the concentration of *Betula* pollen grains in the sediment (Fréchette, unpublished). Shrub birch is known to produce smaller pollen grains than tree birch. The strong correlation between larger *Betula* pollen and higher *Betula* pollen concentrations through the core suggests that during Unit 5oc tree birch grew on the 'Mitten Peninsula'.

(*seda*DNA) in the interglacial units. Holocene midges record cold conditions at Holocene deglaciation (~11.6 ka) but a rapid transition to peak Holocene warmth by 10.5 ka followed by cooling after 8 ka (Fig. 18A). Unit 5 midges show a similar early, rapid summer warming followed by cooling before the midpoint of the unit. Unlike at FOG and BRO, Unit 5 at CF8 does not record midge taxa from south of latitudinal treeline, and peak midge-inferred warmth during the LIG does not exceed that of the early Holocene at this site. Axford *et al.* (2011) speculate that peak Tanypodinae abundance at Lake CF8 might reflect temperatures warmer than during the Holocene. In contrast to the midge results, the flourishing of planktonic diatoms suggests longer open-water conditions during Unit 5 than during the warmest part of the Holocene (Wilson *et al.* 2012). Pollen concentrations are nearly an order of magnitude higher in Unit 5 than in the Holocene (Fig. 18B). Although some of this increase is related to dewatering of Unit 5 gyttja, densification is no more than a factor of two. Both *Betula* and *Alnus* pollen occur at much higher frequencies in Unit 5 than during the Holocene, with *Betula* accounting for ~50% of the early Unit 5 pollen sum, suggesting that dwarf birch may have been growing nearby, and possibly alder was established on southern Baffin Island, whereas there is no evidence that *Alnus* was present on Baffin Island at any time during the Holocene. The presence of *Betula* growing in close proximity to Lake CF8 is confirmed by *seda*DNA (Crump *et al.* 2021). *Seda*DNA and pollen (Fig. 19A and B) analogues suggest peak summer temperatures during Unit 5 were at least 3°C higher than peak early Holocene summer temperatures.

Diatoms (Wilson *et al.* 2012) and an impoverished midge fauna (Axford *et al.* 2009b) in Unit 3 record uniformly cold summers, but the lake was not covered by glacier ice and must have experienced adequate light transmission for chironomid larvae, periphytic and benthic diatoms, and aquatic mosses to maintain viable communities for a brief interval prior to 40 ka.

Midge and pollen assemblages in Unit 7 (Fig. 18) infer summer temperatures and lake water pH similar to the late Holocene. Both proxies register strong cooling into glacial-like conditions at the top of Unit 7. *Seda*DNA was not found in Unit 7 sediment in the 2019 core (Crump, unpub. results).

Despite their antiquity, midge, diatom and pollen assemblages at Lake CF8 have secure modern analogues in calibration datasets for all levels (Axford *et al.* 2011; Wilson *et al.* 2012, Fréchette *et al.* 2008b; Crump *et al.* 2021), supporting the utility of these palaeobiological indicators to assess multiple past interglacial periods. Also of note, Units 7, 5 and 1 all followed a similar pattern of lake ontogeny and establishment of lake biota, despite intervening continental glaciations – the exception being the unique combination of changes within the past century that demarcate the Anthropocene (Axford *et al.* 2009a; Wilson *et al.* 2012).

Lake Attata (ATA) (unpublished)

Lake Attata, a small (4 ha) kettle lake 1 km northwest of Lake CF8, with a water depth of ~10 m was cored in 2007 and 2019. Cores recovered in 2007 and in 2019 have similar stratigraphies to Lake CF8, (Fig. 17D). The three pre-Holocene interglacials (Units 3, 5, and 7; Fig. S2) are separated by coarse sandy units deposited rapidly during deglaciation, when Laurentide meltwater streams briefly occupied ATA's small, steep catchment. Unit 3 consists of 10 cm of nearly pure

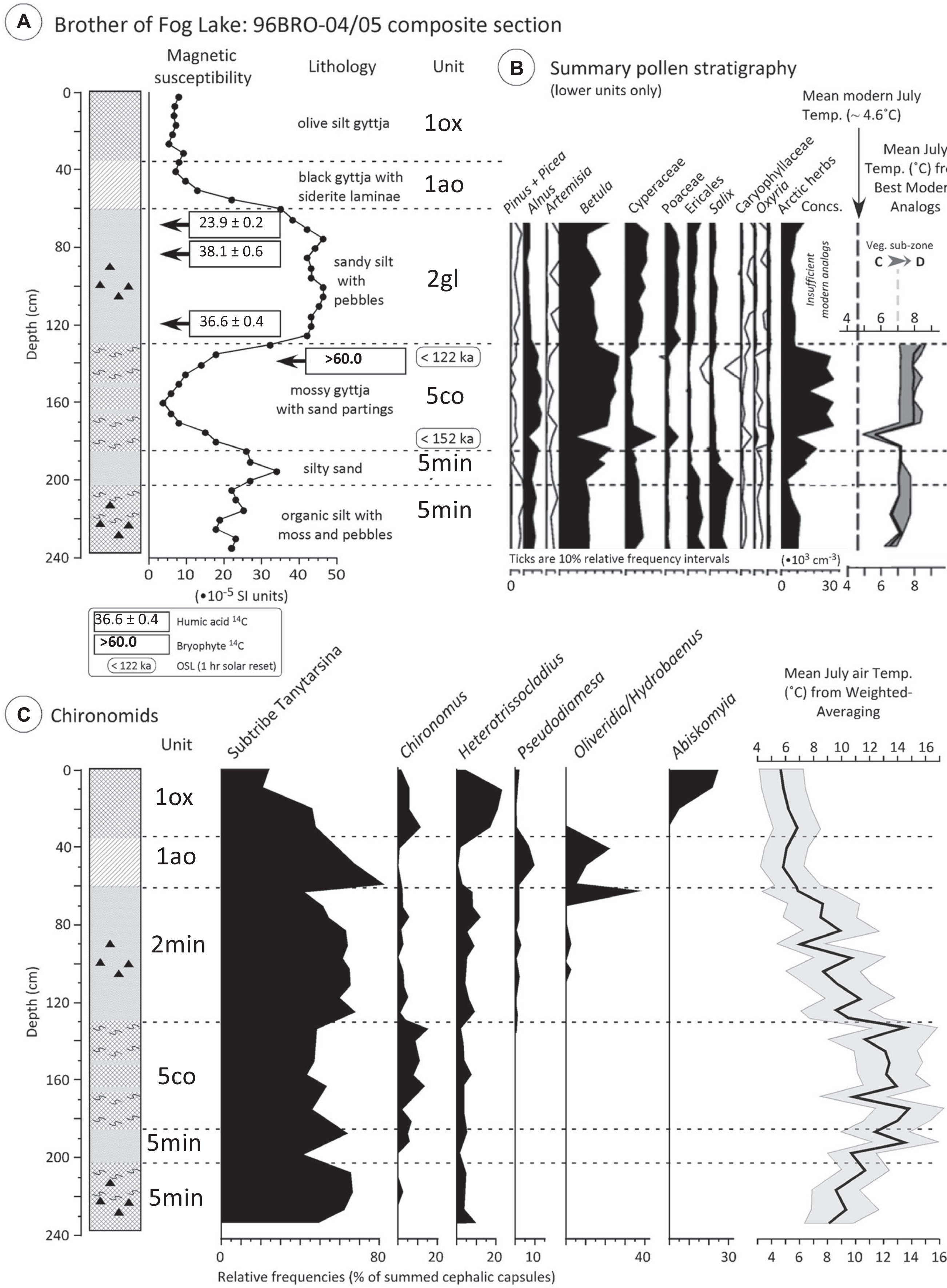

Figure 15. Brother of Fog Lake. A) Core log for composite core 96BRO-04 (Holocene) and 96BRO-05 (pre-Holocene) with key cal ^{14}C dates. B) Palynology of the pre-Holocene units, indicating peak warmth in Unit 5co (Fréchette *et al.* 2006). C) Chironomid taxa from the full composite core, with derived mean July temperatures indicating Unit 5co is the warmest, with mean July temperatures 7°C above mean Holocene July temperatures (Francis *et al.* 2006).

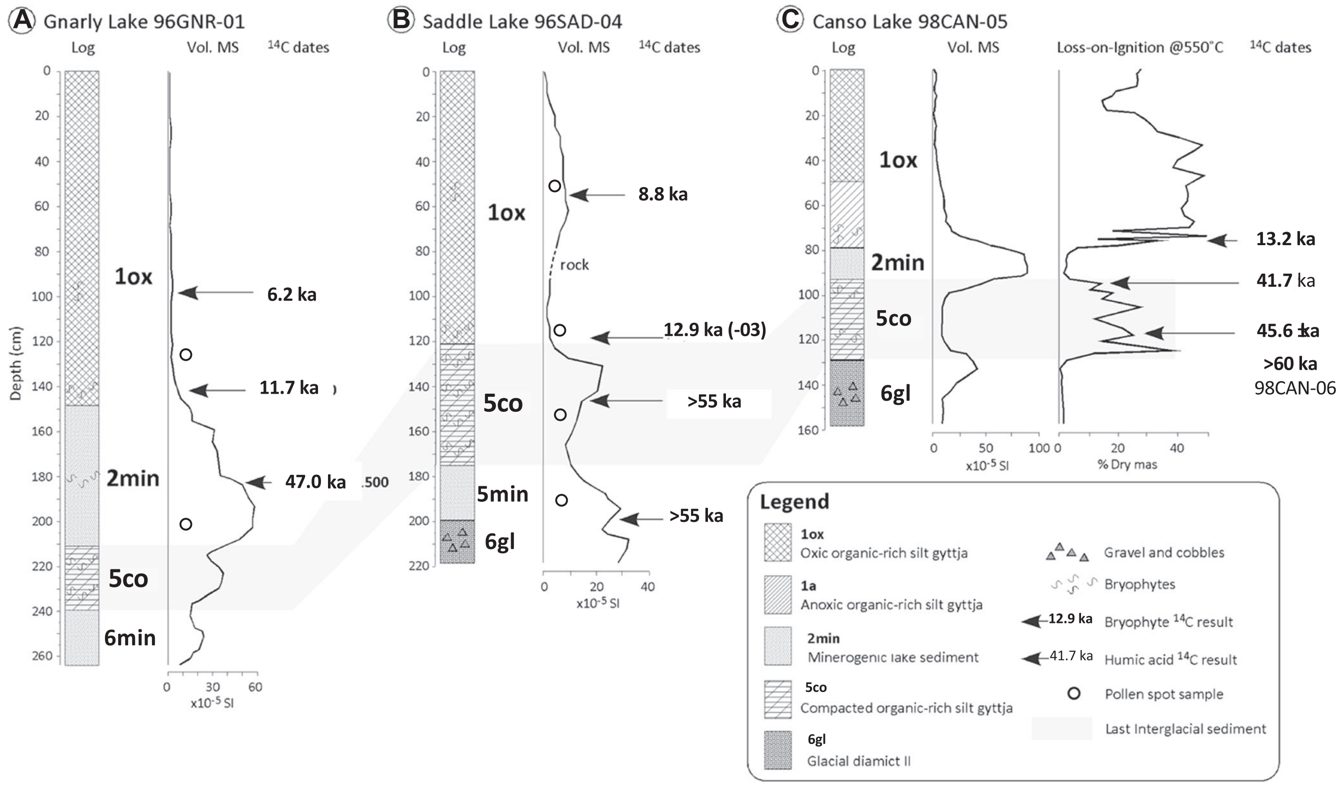

Figure 16. Core logs, magnetic susceptibility and calibrated ^{14}C ages for the key cores from lakes Gnarly, Saddle and Canso, each with compact gyttja at or beyond the range of ^{14}C dating in the deeper portions, either directly below less compact gyttja of Holocene age, or separated from Holocene gyttja by deglacial minerogenic sediment.

aquatic moss, with ^{14}C dates from the 2007 and 2019 cores of 42.9 ka and 44.8 ka, respectively. Unit 5 has a ^{14}C date on aquatic moss of 43.5 ka (Table S1).

Spot Lake (SPT) (unpublished)

Spot, the smallest (1 ha) of the kettle lakes, and situated between CF8 and ATA was cored for the first time in 2019. The bathymetry is conical with a central depth of just over 13 m, unusually deep for such a small lake, but consistent with a kettle origin. Five sediment cores obtained in 2019 from the central deep revealed 145 cm of Holocene gyttja, of which the lower 25 cm are finely laminated black mud, indicative of anoxia. Holocene gyttja is underlain by ~30 cm of well-sorted sand, below which is 12 cm of nearly pure compact aquatic moss, underlain by 60 cm of sand, with at least 16 cm of gyttja below the sand (Fig. 17D). We consider the basal gyttja, extending to at least 268 cm depth in the core, to be Unit 5co. We encountered large stones in some of the coring drives, probably due to allochthonous transport down the steep bathymetric gradient. The stratigraphic succession is similar to the three youngest interglacial units in adjacent lakes CF8, DRP and ATA.

Drop Lake (DRP) (unpublished)

Drop Lake is also a small (4 ha) kettle lake, 3 km south of Lake CF8, with a maximum water depth of 11 m cored in 2019. A composite record was derived by combining a 131 cm surface core of finely laminated Holocene gyttja overlying 29 cm of well-sorted coarse sand, with 280 cm of sediment recovered using aluminium core pipe that by-passed the Holocene before starting to core. On recovery, the leading edge of the aluminium core barrel was dented, indicating the core was terminated by a rocky substrate. Mass MS, water content (not shown) and visual observation provide a composite record of ~4 m (Fig. 17D). The lowest 40 cm are gyttja, with low MS and common moss macrofossils. We consider this unit to be correlative with Unit 5co in nearby Lake CF8, and a 9 cm-thick mossy unit at 180 cm composite depth correlates with Unit 3co in Lake CF8 with a moss ^{14}C date of 45.0 ka.

The preservation of multiple nearby lakes with pre-Holocene interglacial sediment probably stems from their location in a valley at right angles to regional ice flow, either in the Ayr Lake valley to the north or through Clyde Inlet to the south. Briner *et al.* (2005) mapped features in this 'inter-lobate' zone attributed to frozen-bedded conditions.

Africa Lake (AFR) (unpublished)

Africa Lake is the coldest, highest and northernmost of the Baffin Island lakes described here. Situated at 895 m asl in crystalline bedrock at the northern end of Baffin Island, AFR (21 ha) has a central depth of 15 m, and is dammed by a kame terrace deposited at the margin of a northeast-flowing Laurentide outlet glacier (Fig. 8H). A piston core from the central deep, 19AFR-05, recovered 89 cm of sediment (Fig. 17E). The upper 72 cm are Holocene gyttja, except a coarse sand layer 5–10 cm below the core top, with only unconsolidated watery gyttja above it. Below the Holocene gyttja are 17 cm of consolidated gyttja, from which small aquatic moss fragments have ^{14}C ages of 40.3 and 40.5 ka. Five ^{14}C dates on Holocene aquatic moss indicate deposition between 9 ka and 3.5 ka. After 3.5 ka a local ice cap apparently expanded across the lake (neoglaciation), shutting down sedimentation and biological productivity. The lake remained isolated from the atmosphere until the last century, when modern warming resulted in deglaciation.

Unusual geochemical conditions dissolved all diatoms in the Holocene sediment, although biogenic silica is present in

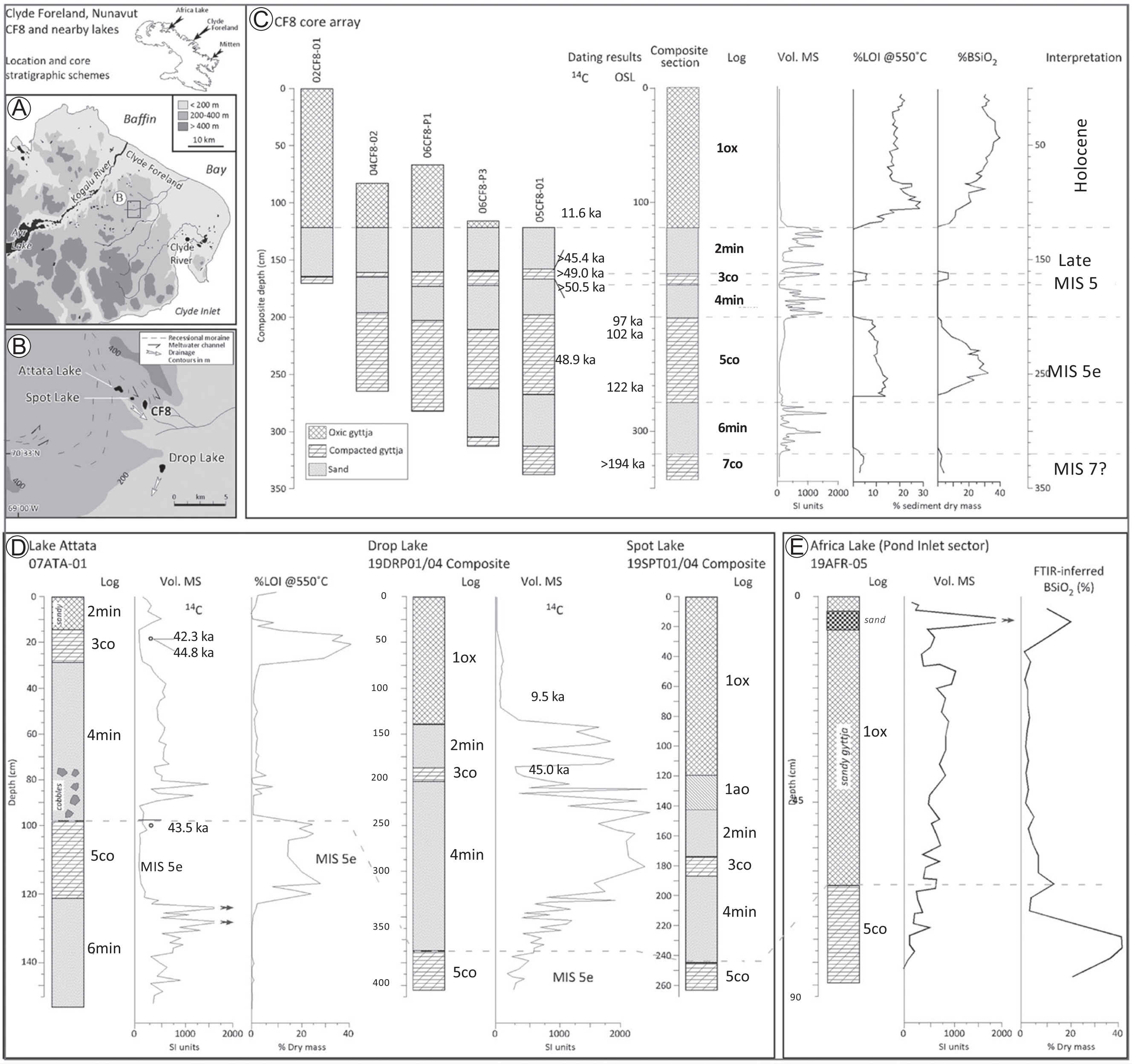

Figure 17. Sediment cores from four nearby lakes (Panels A and B, and Fig. 6B) 20 km inland from the settlement of the Clyde River. Panels C and D show that all four lakes reveal a similar stratigraphic succession, despite each having separate catchments, lending support to the view that the sediment succession captures all lake ice-free intervals since deposition of Unit 7. From the surface downward, all four lakes include gyttja, commonly anoxic at deeper levels, spanning the past ~12 ka, underlain by minerogenic deglacial sediment, likely deposited rapidly (years to decades based on narrow hillside catchments), then a thin layer of mossy gyttja (3co) with ^{14}C ages at or beyond the reliable range of the method, and underlain by minerogenic deglacial sediment, similar to Unit 2, and thought to be deglacial prior to Unit 3co. Beneath which is a relatively thick unit of compact gyttja (5co), with OSL ages consistent with a Last Interglacial (MIS 5e) age, and with a total mass similar to that of Holocene gyttja. In lakes Attata and CF8 Unit 5co is underlain by minerogenic deglacial sediment, which in lakes CF8 and ATA (2019 core) is underlain by compact silty gyttja (7co), with OSL ages suggestive of an MIS 7 or older age. E) Sediment log for core 19AFR-05, with an upper gyttja unit overlying a denser gyttja, but with less clastic sediment. ^{14}C dates on composite rare moss fragments are >40 ka, and we tentatively correlate this with Unit 5 at CF8.

significant concentrations. Diatoms are abundant, and well preserved below 72 cm. *Sed*aDNA analyses from 15 levels, including three through the interglacial, did not produce identifiable plant DNA (Crump, unpub.), but the process used is specific to vascular plants, which are rare at this elevation.

Wax Lips Lake (WLL), northwest Greenland (McFarlin et al. 2018)

Wax Lips Lake (9 m deep, ~7 ha, 517 m asl) is currently only 2 km from the margin of the Greenland Ice Sheet. WLL is inset into a broad shelf ~100 m above an adjacent valley through which a Greenland Ice Sheet outlet glacier flowed to the sea, ~25 km distant (Fig. 8A). The landscape around WLL is characterised by angular boulder fields and weathered tors, geomorphological footprints of cold-based ice. Cosmogenic nuclide inheritance in nearby bedrock (Farnsworth *et al.* 2018) is consistent with a cold-based and minimally erosive Greenland Ice Sheet in the vicinity of WLL.

Sediment cores obtained from WLL in 2012 and 2014 recovered up to 220 cm of stratified sediment, almost entirely gyttja, containing abundant aquatic moss (Fig. 20). A clear boundary in sediment colour, density and MS at ~165 cm depth separates Holocene gyttja (Unit 1) with a basal age of 10 ka from the underlying denser, dewatered gyttja (Unit 5co) with non-finite ^{14}C ages on aquatic moss (Table S1).

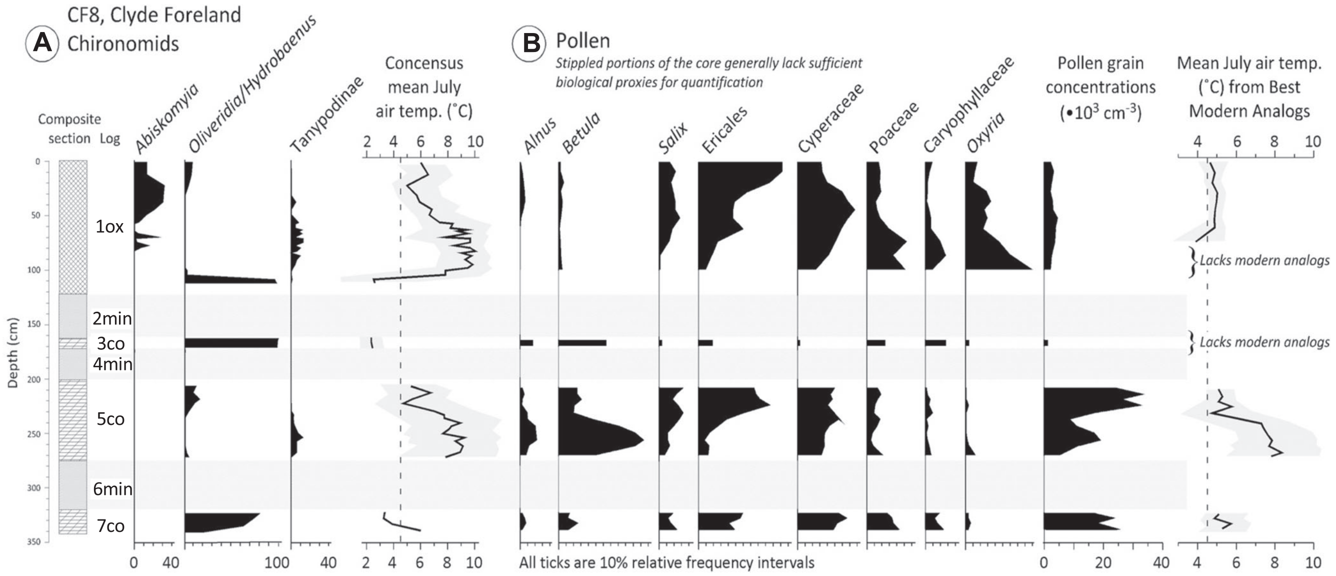

Figure 18. Summary chironomid and pollen diagrams for the four interglacial beds in Lake CF8. Although the chironomids do not show the Unit 5co to have been significantly warmer than present, the pollen does. Both chironomid and pollen data indicate that interglacials 3co and 7co were cooler than the Holocene. Modified from Axford *et al.* (2011) and Crump *et al.* (2021).

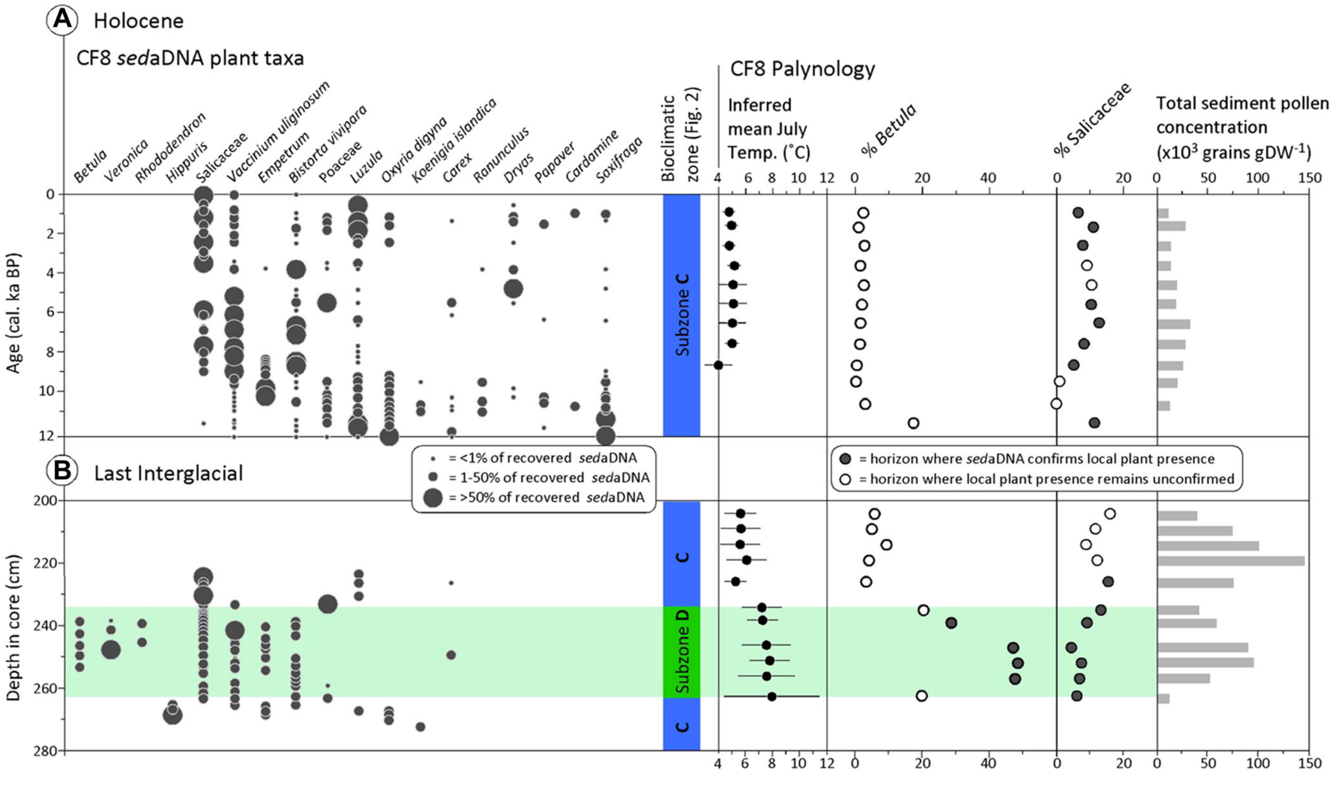

Figure 19. Clyde River Lake CF8 showing summary *seda*DNA and palynology in Holocene (A) and Unit 5co (B) sediment. Holocene *seda*DNA is from core CF8-17-03 and the Unit 5co *seda*DNA is from core 19CF8-07. Key pollen taxa, inferred pollen July temperature and pollen concentrations for the Holocene and Unit 5co beds is from CF8 cores from 2002 and 2006. The pollen and DNA cores are correlated using age–depth models for the Holocene, and bulk geochemical trends in Unit 5co (independent of DNA and pollen; see Crump *et al.* 2021 for details). The intervals in Unit 5co sediment with *Betula* DNA present in the 2019 core, align with intervals of high *Betula* pollen percentages and concentrations in previous cores. Holocene sediment revealed no *Betula* DNA and almost no *Betula* pollen except in the oldest level, which we expect to be reworked from interglacial soils as pollen concentrations are extremely low. [Color figure can be viewed at wileyonlinelibrary.com]

Chironomids (Fig. 20B) are abundant throughout the Holocene gyttja, and reveal a major species assemblage shift from relatively warm-adapted species towards cold-adapted species between the early and late Holocene, with an inferred overall Holocene summer cooling of 5.5 ± 1.7°C. Unit 5co sediment contains chironomids and *Chaoborus*; the latter is presently extralimital, absent from early Holocene sediments in Greenland, but common in lower latitudes of Canada today and rarely found north of the modern boreal treeline. The most warmth-demanding assemblages from the Unit 5co gyttja imply summer temperatures 7.0 ± 1.7°C warmer than today, warmer than the early Holocene.

Unlike most sites on Baffin Island, there is no distinct minerogenic layer between Units 1 and 5 at WLL, although

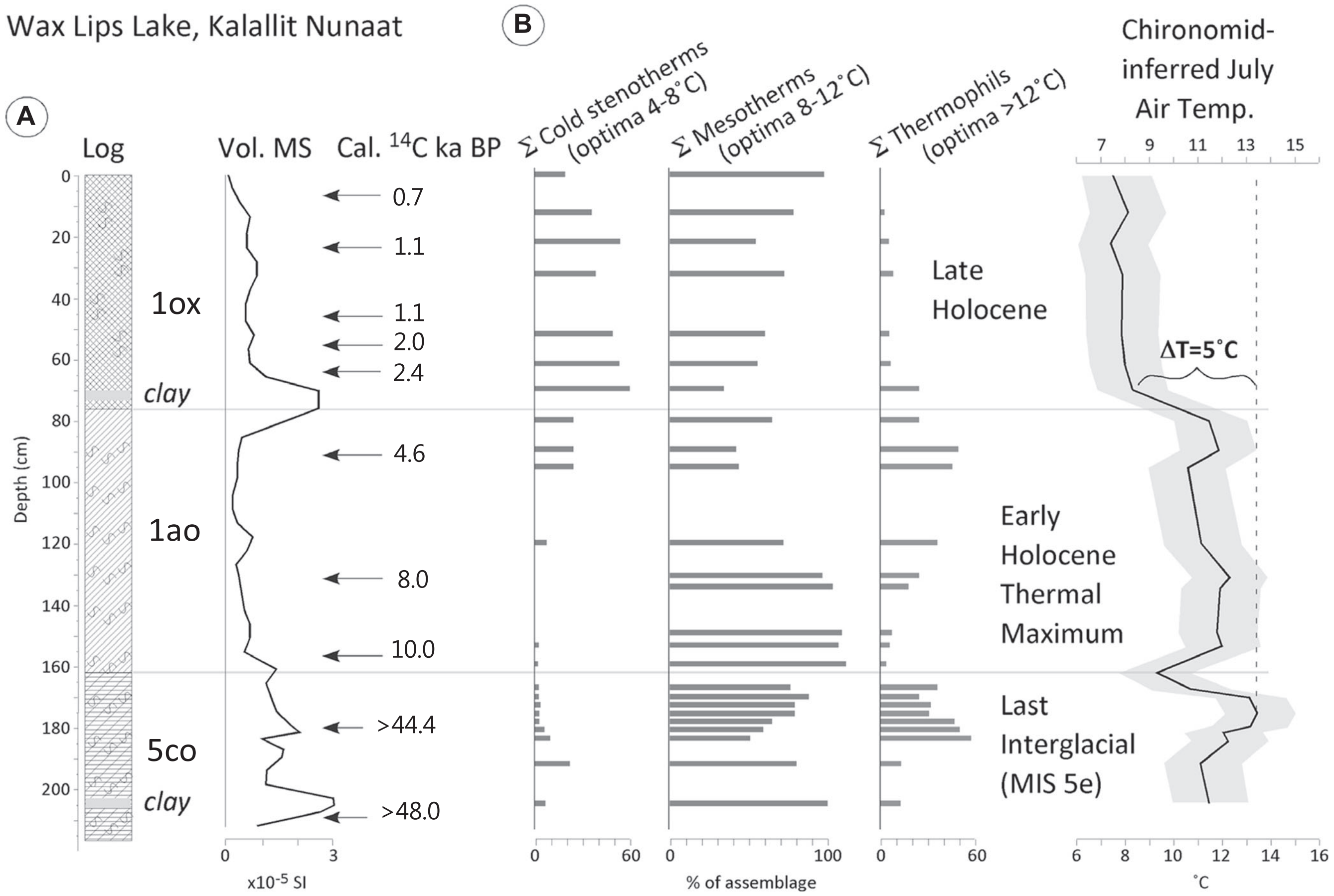

Figure 20. Summary sediment log, ^{14}C ages and chironomid taxonomy and reconstructed July air temperature for Wax Lips Lake (WLL), northwest Greenland, showing 5°C warmer temperature during the Last Interglacial relative to the Holocene (modified from McFarlin *et al.* 2018).

clastic grains do increase within the top of Unit 5co. Plausibly, the lake's limited catchment, and its location on a plateau immediately adjacent to a trough, may have sheltered it from meltwater sedimentation during deglaciation.

Discussion

Ages of units

All 13 lakes have unique catchments; none of the lakes receive drainage from a lake higher in the same drainage.

Unit 1 is gyttja, radiocarbon-dated to be wholly deposited during the Holocene, after meltwater from the receding ice sheets exited each lake's catchment.

Unit 2 is interpreted to have been deposited during LGM deglaciation, while ice-sheet meltwater remained in the catchment. At lakes RL, SAD, AFR and WLL, catchment/ice-sheet relations are such that no significant deglacial sediment was deposited in the lakes. For lakes CF8, ATT, SPT and DRP, deglacial meltwater deposited only well-sorted sands lacking datable material, probably reflecting a brief interval of channel-constrained meltwater in their catchments. At the remaining lakes (AKL, FOG, BRO, GNR and CAN) Laurentide meltwater probably remained in the catchment for a considerable interval, eroding ancient catchment soils and delivering poorly sorted mineral sediment containing mixtures of ancient (>40 ka) and contemporary organic remains to the depocenter. FOG provides the best example of the latter setting, where five ^{14}C dates on macrofossils range from 8.9 ka to 36.8 ka and four on humic acid extracts range from 9.1 ka to 19.4 ka through 30 cm of Unit 2, with no correlation to depth or each other (Fig. 13). Their reworked origin is supported by the pollen records showing higher pollen concentrations in Unit 2 (30k grains cm^{-3}) than in Holocene gyttja (5k grains cm^{-3}), dominated by alder and birch pollen, despite the chironomid record, which is aquatic in origin, so not washed in, that is dominated by *Oliveridia*, a taxon indicative of a cold, high-sedimentation-rate environment. *Oliveridia* disappears from the record at the Unit 2/1 transition. Importantly, there are almost no Unit 5 chironomid taxa (other than the ubiquitous Tanytarsina subtribe) in Unit 2, consistent with Unit 2 pollen being derived from catchment soil erosion, and not reworked lake sediment. Similar details characterise Unit 2 in Lakes AKL, BRO and GNR. Richard et al. (1991) reach a similar conclusion of reworked older pollen in deglacial sediment from Ungava, Canada. We consider the depositional age of Unit 2min in all settings to be early Holocene, only a few decades to centuries older than the base of Unit 1. All lakes become free of ice-sheet influence ~11 ka, or shortly thereafter, with an abrupt transition to gyttja sedimentation.

Unit 3 is only present in the Clyde lakes (CF8, ATA, DRP and SPT), where it is always a thin (~10 cm-thick) moss-rich unit bounded by well-sorted deglacial sands. Seven ^{14}C dates on Unit 3 moss are all >40 ka; the oldest is >50 ka. The few climate proxies suggest summer temperatures colder than the Holocene. The lack of similar units in our other lakes suggest Unit 3 represents a modest deglacial event that only uncovered the Clyde lakes before Laurentide ice readvanced, sealing the lakes again until the early Holocene. We suggest a likely age of MIS 5a or 5c, implying no major Laurentide deglaciation since MIS 5. With the assumption that Laurentide deglaciations follow similar patterns, and given that the

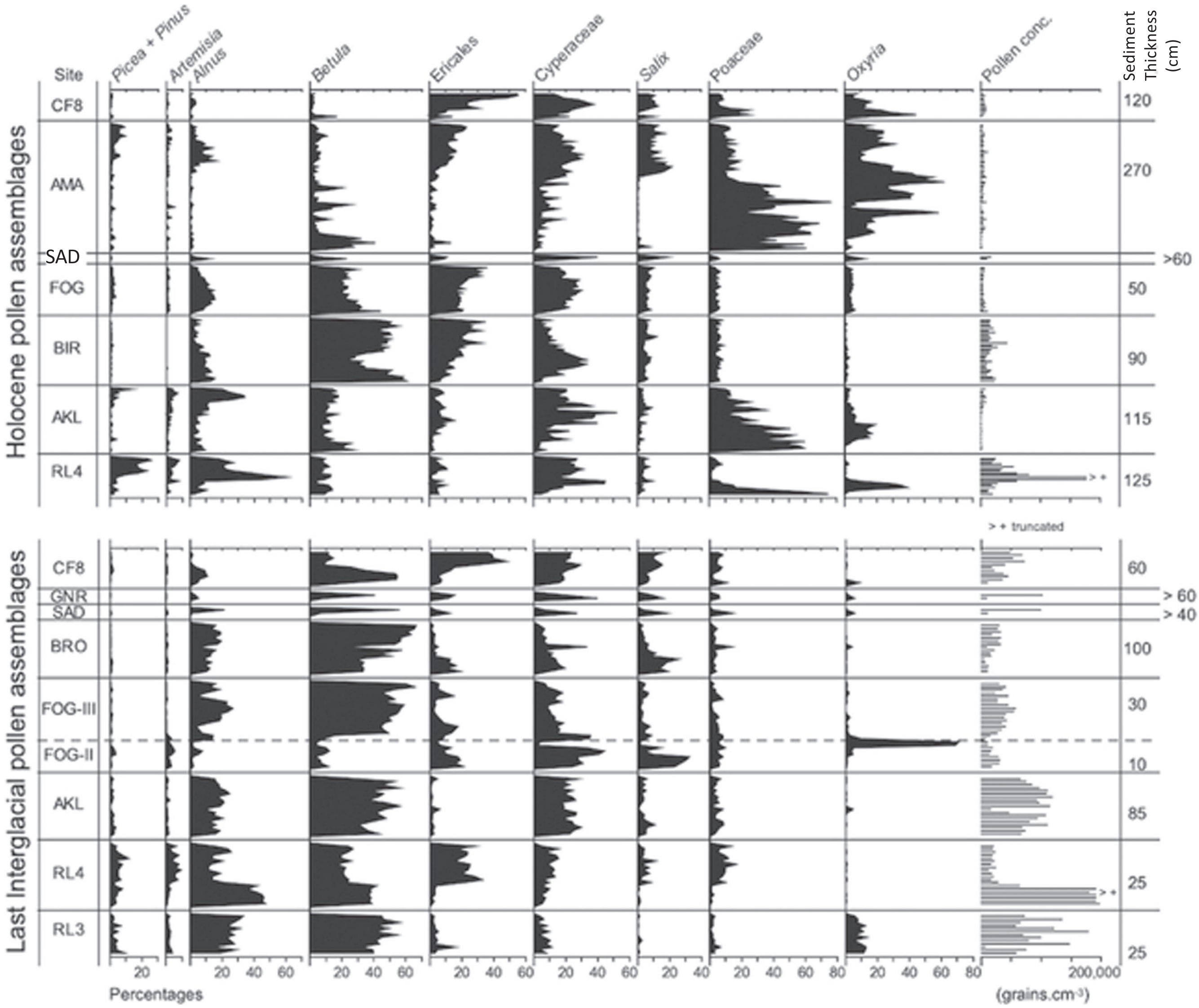

Figure 21. Composite pollen diagrams from Baffin Island lake sediment cores illustrating the consistent differences in pollen concentrations and pollen relative abundances between Holocene sediment (Unit 1ox; upper panel; see also Fig. S1) and Last Interglacial sediment (Unit 5oc; lower panel), both ordered with most southerly sites at the bottom, and northerly at the top. Holocene pollen concentrations are much lower than in Last Interglacial sediment, and the relative abundances of *Betula* and *Alnus* are higher in the Last Interglacial than Holocene sediment. The two modest exceptions are Akvaqiak Lake (BIR), a lake in a warm microclimate with abundant, tall, dwarf birch shrubs (Fréchette, 2007) and RL4, from Robinson Lake, our southernmost site. With the exception of BIR, *Betula* and *Alnus* pollen percentages are low in Holocene sediment, but dominant in the LIG sediment.

Clyde lakes were depositing gyttja before 11.6 ka, this suggests that the LIS remained largely intact from >50 ka until the early Holocene.

Unit 5co is present in all 13 lakes described herein. In all lakes, Unit 5 is the first gyttja-dominated unit below Holocene mud, with climate proxies indicative of summer temperatures above peak Holocene warmth. Unit 5 radiocarbon dates are available from all 13 lakes, and all of those dates, including humic acid extracts, are >40 ka ($n = 35$; Table S1). We conclude that Unit 5 is beyond the range of ^{14}C dating. Given these similarities, we consider Unit 5 correlative across all 13 lakes. Luminescence dating was attempted on Unit 5 sediment from four lakes: RL, FOG, BRO and CF8. Ten analyses (TL and IRSL) from three levels in Unit 5 sediment from RL averaged 84 ± 10 ka, sufficient to confirm an MIS 5 age but insufficiently precise to determine which substage in MIS 5. Four IRSL ages from Unit 5 at FOG, averaged 95 ka, whereas two TL ages averaged ~86 ka, again clearly indicating an MIS 5 age but with considerable uncertainty. OSL ages, considered more reliable for sediment dating than TL or IRSL, from the top of Unit 5 at CF8 are 97 ± 10 ka and 105 ± 10 ka, whereas basal Unit 5 sediment has an OSL age of 122 ± 12 ka, indicating that Unit 5 was deposited early in MIS 5. The OSL signal in silt from Unit 7 is >194 ± 19 ka, suggesting an MIS 7 age.

The most compelling line of evidence that Unit 5 is correlative with MIS 5e comes from the pollen data. We reiterate the argument first articulated by Fréchette (in Miller *et al.* 1999) that the record of *Alnus* pollen in Unit 5 requires that when Unit 5 was being deposited the LIS was at least as small as it was ~7 ka. *Alnus* is not known to have grown on Baffin Island during the Holocene, but is common in northern Labrador/Quebec, and *Alnus* pollen is efficiently wind transported. *Alnus* pollen first appears in postglacial northern Labrador lake sediment records ~8 ka, reaches peak abundance ~6.5 ka, declining after 6 ka (Short and Nichols, 1977; Lamb, 1985). This sequence is matched in timing and trends in changes of *Alnus* pollen percentages in Holocene sediment from Baffin Island lake cores 91-RL4 (Fig. 10), 96FOG-05 (Fig. 13) and 95DON-03, 95DLW-03 (Fig. S1). Because the Holocene *Alnus* pollen percentages in Baffin Island lakes faithfully mirror the *Alnus* percentage in

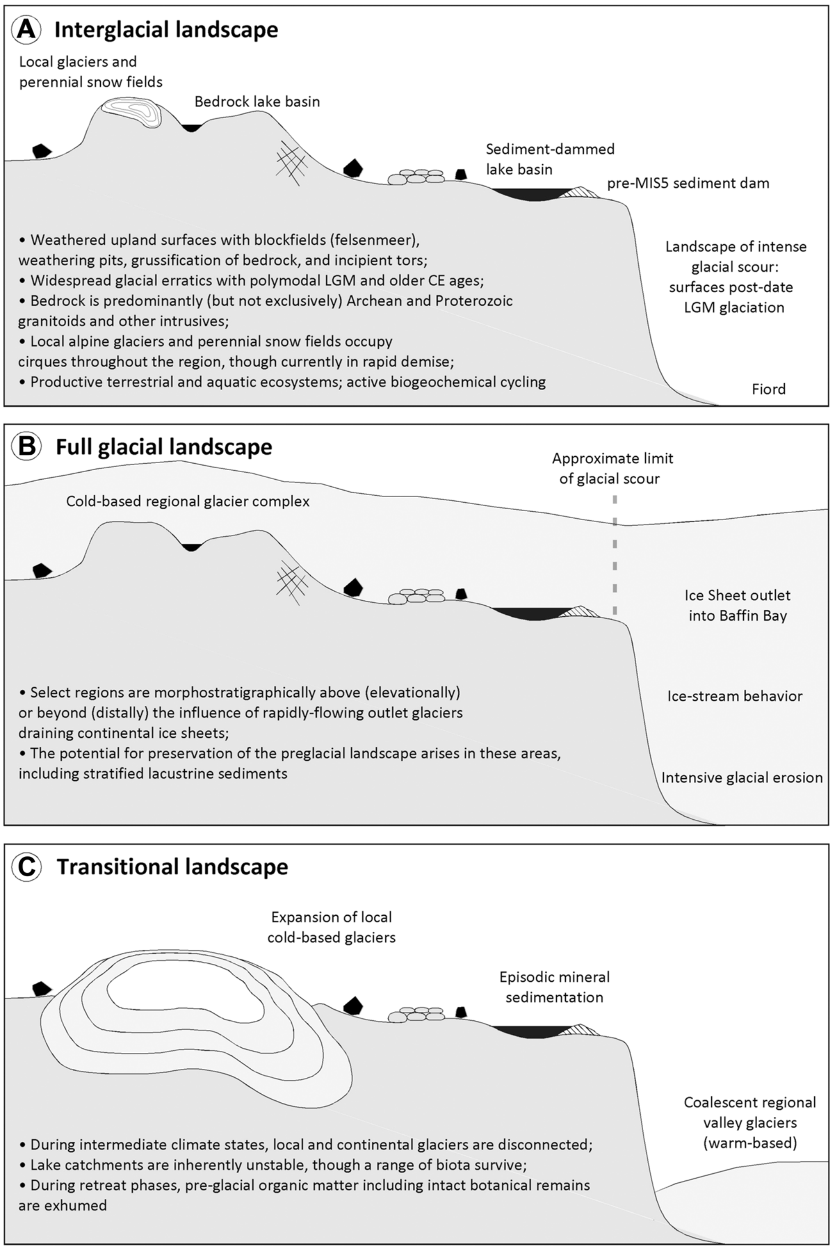

Figure 22. Schematic cross-section of a glaciated landscape with steep-walled deep fjords that extend as connecting valleys reaching into the interior of Baffin Island, and relatively low-relief interfluves that support independent glaciers. A) Lake basins created by a sediment dam during deglaciation acquire gyttja sediment; erratic boulders deposited by the last glacial cycle begin to acquire cosmogenic radionuclides (CRN). B) The same landscape under full glacial conditions with thick, relatively fast-moving erosive outlet glaciers in the fjords, and thinner, cold-based ice mantling the interfluves. Erratic boulders remain in place, but their CRNs decay and no new production. C) Transitional (neoglacial) landscape, with local glacier expansion, additional gyttja sedimentation in the lake, and additional CRN production in erratic boulders, resulting in apparent ages much younger than depositional ages, but with a measurable disequilibrium in their concentrations.

lakes from their source area of northern Labrador/Quebec, we argue that Baffin Island *Alnus* pollen percentages in older interglacials similarly reflect the status of *Alnus* tree status in northern Labrador/Quebec. Consequently, we conclude that the high concentrations and high relative percentages of *Alnus* pollen in Unit 5co in Baffin Island lake sediment documented herein, are derived from northern Labrador/Quebec, which requires the Labrador Dome of the LIS to have deglaciated, and northern Quebec to have been ice-free. Based on the timing of Laurentide MIS 1 deglaciation (Dyke, 2004), the Labrador Dome deglaciates from most of northern Quebec ~7.5 ka, when eustatic sea level was within 10 m of the present (Chappell *et al.* 1996; Grant *et al.* 2014). Consequently, assuming similar deglacial patterns, the high levels of *Alnus* pollen in Unit 5co sediment from Baffin Island lakes must have occurred when sea level was within 10 m of the present. The most recent time prior to the Holocene when sea level was within 10 m of the present was during the LIG, MIS 5e, 130–115 ka, from which we conclude that Unit 5co in our 12 Baffin Island cores, and by correlation, the northwest Greenland lake, WLL, was deposited during that interval.

Inferences of climate evolution since MIS 6 deglaciation

Comparisons between LIG and Holocene summer temperatures are derived from pollen, chironomids, diatoms and *sed*aDNA. In almost every case, summer temperature proxies indicate peak warmth during the LIG was significantly higher than at any time in the pre-industrial Holocene. Quantitative estimates suggest peak LIG summer temperatures 4–6°C higher than pre-industrial, probably accompanied by a longer open-water season. We argue that anomalous LIG warmth apparent across a 1500 km transect through the eastern North American Arctic, was in response to an orbitally driven summer insolation anomaly 3% higher than the peak early Holocene anomaly, which, combined with early MIS 6 deglaciation resulted in Northern Hemisphere ice sheets close to modern dimensions by the time orbitally driven summer insolation reached its maximum (Fig. 1). The insolation anomaly was probably intensified by diminished summer albedo and greater moisture fluxes to the atmosphere linked to reduced summer and winter sea ice, higher sea-surface temperatures, a shorter snow-cover season, poleward expansion of shrubby plants, and permafrost thaw (Arctic amplification). The timing and magnitude of the insolation anomaly relative to MIS 6 deglaciation intensified by Arctic amplification, provide mechanisms to help explain the observed LIG Arctic summer warmth, with implications for a similar response to anticipated greenhouse warming in the near future.

A schematic representation of lake and ice-cover history from the LIG to the late Holocene is provided in Figures 5 and 22. Although most records reveal an increase in clastic sediment toward the end of the LIG, the lack of a strong transition from gyttja to dominantly clastic sediment at the end of the LIG suggests that lake surface waters froze permanently before glacier ice and associated summer meltwater entered their catchments, or, less likely, there was no meltwater, even in summer. However, the common occurrence of deglacial clastic sediment prior to deposition of Holocene gyttja (Unit 2min in FOG, BRO, CAN, GNR, CF8, DRP, SPT and ATA) suggests that an 'interglacial climate' was established prior to LGM catchment deglaciation. We conclude that all lakes were deglaciated during 'warm' times, and that the presence and nature of deglacial clastic sediments depends largely on catchment features that govern whether those sediments were sorted sand, poorly sorted glacially derived sediment, or reworked catchment soils. Once meltwater departed the lake's catchment, the minerogenic component declined abruptly, with gyttja-dominated lake sediment preserving reliable proxies and radiocarbon ages.

Inferences on ice-sheet dimensions and global sea level during the last glacial cycle

Lakes record sedimentation whenever they are at least seasonally ice-free. In eight of the lakes described here (FOG, BRO, GNR, CAN, CF8, ATA, DRP and SPT), Holocene gyttja is underlain by clastic-dominated sediment of variable thickness and character, deposited rapidly during deglaciation of the lakes' catchments (Unit 2min). This replicated succession suggests that the lakes deglaciated during warm summers when ice sheets produce copious meltwater as the ice margin recedes through lake catchments, with the nature of the sediment highly dependent on catchment morphometry and sediment availability. In two lakes, (RL and AKL) a diamict separates Unit 1 from older gyttja, and in the other three lakes (WLL, SAD and AFR), gyttja of Units 1 and 5 lack any intervening sediment. These differences probably reflect variations in the relationship between lake position and deglacial pathways.

The sediment we interpret to have been deposited during the LIG (Unit 5co) has been shortened in thickness by slow dewatering from the weight of overlying sediment, but the LIG mass accumulation is similar to the mass accumulation during the postglacial interval, suggesting that they represent similar time intervals. We conclude that during the last deglaciation, lakes fringing Baffin Bay were seasonally ice-free and began accumulating sediment 10–12 ka, at a time when the LIS remained largely intact with glacial ice over its core sector in Hudson Bay (Dyke, 2004), and sea level was 40–60 m below the present-day level (e.g. Waelbroeck *et al.* 2002). Assuming LIS recession follows a similar pattern during each deglacial cycle, the lack of organic-bearing material between the LIG and Holocene intervals in the sediment sequences (except the four adjacent Clyde lakes) implies that the LIS never receded behind its 10 ka margin between ~115 ka and ~10 ka, while sea level probably remained 40 m or more below the modern level.

The interpretation of cosmogenic radionuclide inventories in erratic boulders is informed by lake records

Well over a thousand cosmogenic nuclide inventories have been measured in erratic boulders and bedrock surfaces over the past 25 years from across fjord terrains on Baffin Island and Greenland. These data have informed our understanding of both ice-sheet history over the last glacial cycle and the spatial patterns of glacial erosion vs. glacial protection. However, many of these samples have greater nuclide inventories than are possible for exposure exclusively since the last deglaciation. In landscapes repeatedly occupied by non-erosive ice, rock surfaces are alternately shielded from, and exposed to, cosmogenic nuclide production. Thus, in these locations, rock surfaces exposed following LGM deglaciation may contain inventories that have equivalent ages much greater than postglacial exposure. Interpreting the exposure history for such samples is challenging. By measuring two cosmogenic isotopes with very different half-lives, such as ^{10}Be and ^{26}Al, if their isotopic concentration ratios differ from their established production ratios, this would confirm that the rock surfaces experienced differential decay during prolonged burial beneath glacial ice. However, the sensitivity of this particular isotope pair is such that the minimum duration of burial required to be detectable is more than 100 kyr. For example, if adjacent till boulders have ^{10}Be and ^{26}Al inventories indicative of ~30 ka exposure, and isotopic concentration ratios consistent with their production ratios, it is equally plausible that the boulders were deposited during MIS 6 deglaciation, exposed during MIS 5e, then continuously ice-covered until LGM deglaciation, and continuously exposed subsequently, as that they represent a very different exposure history such as MIS 4 deposition and MIS 3 exposure before LGM reburial and postglacial exposure.

Given that intervals of lacustrine sedimentation define ice-free periods between episodes of frozen-bedded glacial overriding, and assuming that the 13 lakes discussed herein are representative of regional ice-cover histories, our lacustrine sedimentary record indicates that most of Baffin Island (except the Clyde River lakes) and northwest Greenland were continuously glaciated from the end of the LIG until the early Holocene. Consequently, rock surfaces across those regions were almost certainly shielded from the flux of cosmic rays by cold-based overlying ice >30 m thick throughout that interval. With this constraint, rock surface cosmogenic nuclide inventories that exceed those from 12 kyr exposure reflect exposure only during MIS 5e (and/or earlier interglacials) and MIS 1. For example, two adjacent moraine boulders by FOG reported by Steig *et al.* (1998) with ^{10}Be exposure ages of 35 and 36 ka and ascribed to a MIS 3 glaciation, are more likely to have experienced ^{10}Be and ^{26}Al production *only* during MIS 5e and MIS 1. Their current ^{10}Be and ^{26}Al inventories are consistent with their deposition during MIS 6 glaciation, rather than a glaciation event within the last glacial cycle. This interpretation differs from that proposed by Steig *et al.* (1998), but is internally consistent with both isotopic concentrations and isotopic ratios. Similar reinterpretation of many ^{10}Be-dated erratics from Arctic Canada and Greenland with apparent ages between 15 and 40 ka is possible if they have been continuously ice-covered since MIS 5e.

Optimal characteristics for preservation of ancient sediment in lakes beneath continental ice sheets

Although many lake basins across the glaciated North American Arctic were formed prior to the LGM, sediment that accumulated prior to the LGM was removed from most basins by glacial erosion or high-energy meltwater during deglaciation. The efficiency of glacial erosion is highly correlated with conditions at the bed of the ice sheet; high lake densities have been used to identify former regions of fast-flowing, erosive continental ice sheets (e.g. Andrews *et al.* 1985), whereas large regions along the eastern margin of Baffin Island and western Greenland exhibit geomorphic characteristics consistent with cold-based ice (Sugden, 1978; Briner *et al.* 2006). Below, we summarise the local characteristics most commonly shared among the 13 lakes preserving pre-LGM sedimentary units reported here. Summarising the key factors these lakes share may allow targeted searches for other lakes with pre-LGM sedimentary records within glaciated regions of the Northern Hemisphere.

- The most common shared characteristic is the nature of lake formation. Eleven of the 12 Baffin Island lakes included here are sediment-dammed, either by kame terraces (RL, BRO, SAD, GNR and AFR), moraines (FOG and CAN), or as kettle lakes (CF8, ATA, DRP and SPT). All of these lakes are in valleys at right angles to regional Laurentide ice flow, which results in driving forces for ice velocity primarily related to the slope of the local ice surface.
- All 13 lakes have small catchments, typically less than a few km^2.
- All 13 lakes are situated in physiographical settings that reduce the likelihood of fast-moving or warm-based ice flow during glacial stages, with little evidence of glacial scour, including the presence of weathering pits, quartz-vein relief of several centimetres, macrocrystalline residuum, tors, and occasionally blockfields and felsenmeer.
- Most lakes are inset into landscapes where the surrounding physiography resulted in ice-sheet flow efficiently channelled to the sea through nearby valleys, fjords and sounds.
- Elevation alone does not seem to be a particularly strong predictor for the preservation of ancient sediment, as our lakes range from 160 to 895 m asl.
- Present-day water depth is not an important predictor.

Conclusions

A wealth of palaeoenvironmental information is contained in pre-Holocene lake sediment. Lake sediment preserved beneath cold-based ice-sheet advances on Baffin Island and northwest Greenland reveal that the Last Interglacial peak summer temperatures were 4–6°C higher than the pre-industrial, and probably accompanied by a longer open-water season. Summer warmth was initiated by summer insolation anomalies 12% higher than peak Holocene anomalies and an earlier deglaciation relative to the insolation anomalies than during the Holocene, intensified by Arctic amplification linked to diminished summer albedo over land and sea, poleward expansion of shrubby plants, and permafrost thaw. Although the forcing for LIG warmth differs from current forcings, LIG reconstructions provide important constraints relevant to predictions of changes in the coming centuries. The emerging view of near continuous ice-sheet coverage across large regions of North America throughout the last glacial cycle provides new constraints on ice-sheet behaviour and sea level over the past 130 ka, is consistent with the marine δ^{18}O record across the same interval, and has implications for the interpretation of cosmogenic nuclide inventories and inferred apparent exposure ages in rocks across this region. While the geochronology of pre-Holocene interglacial sediment remains challenging, and rare preservation of ancient *seda*DNA strands of sufficient length may limit its applicable time domain, it is also unquestionable that additional lacustrine localities exist with potentially even longer records of successive interglacial sediment and their associated biomes that await study (Fig. 21).

Acknowledgements. We acknowledge the permission granted to us by the Qikiqtani Inuit to access their Baffin Island homeland for this research, and for their generous advice, assistance and friendship over the past 30 years. Likewise, the people of Kalaallit Nunaat (Greenland) have generously granted us access to their homeland. We also recognise assistance from many graduate and undergraduate students, acknowledged in the individual publications synthesised here, in the field and in our laboratories. The fieldwork that led to the acquisition of the sediment cores described herein, and the analyses that we report, were chiefly sponsored by the US National Science Foundation (NSF), through the Offices of Polar Programs and Atmospheric Sciences, and from sources within the Canadian Government. Initial support that was instrumental in Baffin Island lake-coring was through the PALE (Paleoclimate from Arctic Lakes and Estuaries) initiative at NSF. Significant support came from NSF awards 9122974, 9402657, 9503279, 9526384, 9708418, 9809795, 0455025, 0909347, 1107411, 1108306, 1454734, 1737716, 1652274 and 1737712. Polar Continental Shelf Project, Government of Canada, provided essential logistical air support. Additional support came from other sources awarded directly to individual authors. All support is gratefully acknowledged.

Author contributions—GHM initiated the text and led most of the Baffin Island lake-coring expeditions. JPB led most of the lake-coring near Clyde River, and contributed text on implications for ice flow and cosmogenic radionuclide exposure ages. APW participated in much of the fieldwork, contributed figures, discussions on large-scale ice flow, and interpretation and text related to the sediment core records. He is responsible for the AKL record. BF contributed unpublished pollen records, revised previous pollen figures, and contributed text. DF and YA contributed the Baffin Island chironomid data. SC contributed text and *seda*DNA data, and led some of the fieldwork. HB, DG, JR, MR, JS, ET and GdW assisted the acquisition of Baffin Island cores, generating and interpreting records, and commented on the text. YA, MK, JM, and EO provided the Greenland (WLL) record and contributed to the text. The authors declare no conflicts of interest.

Supporting information

Additional supporting information can be found in the online version of this article.

Figure S1. Pollen records in sediment cores from two lakes near Cape Dyer, Baffin Island, that show the evolution of *Alnus* pollen through the Holocene.

Figure S2. Water content in Lake Attata sediment showing four superposed interglacial units.

Table S1. Data for radiocarbon dates used in this paper.

References

AMAP. 2021. *Arctic Climate Change Update 2021*. Arctic Monitoring and Assessment Programme (AMAP): Tromso.

Andrews JT, Clark P, Stravers JA. 1985. The patterns of glacial erosion across the Eastern Canadian Arctic In *Quaternary Environments: Eastern Canadian*. In *Arctic, Baffin Bay and Western Greenland*, Andrews JT (ed). Allen and Unwin: Boston; 69–92.

Axford Y, Briner JP, Cooke CA *et al.* 2009a. Recent changes in a remote Arctic lake are unique within the past 200,000 years. *PNAS* **106**: 18443–18446.

Axford Y, Briner JP, Miller GH *et al.* 2009b. Paleoecological evidence for abrupt cold reversals during peak Holocene warmth on Baffin Island, Arctic Canada. *Quaternary Research* **71**: 142–149.

Axford Y, Briner JP, Francis DR *et al.* 2011. Chironomids record terrestrial temperature changes throughout Arctic interglacials of the past 200,000 yr. *GSA Bulletin* **123**: 1275–1287.

Berger A. 1978. Long-term variations of daily insolation and Quaternary climatic changes. *Journal of Atmospheric Sciences* **35**: 2362–2367.

Bennike O, Böcher J. 2021. Interglacial Biotas from the North Atlantic Islands. In *Biogeography in the Sub-Arctic*, Panagiotakopulu E, Sadler JP (eds). Wiley, 51–82. https://doi.org/10.1002/9781118561461.ch3

Brigham-Grette J, Melles M, Minyuk P *et al.* 2013. Pliocene Warmth, Polar Amplification, and Stepped Pleistocene Cooling Recorded in NE Arctic Russia. *Science* **340**: 1421–1427.

Briner JP, Miller GH, Davis PT *et al.* 2005. Cosmogenic exposure dating in arctic glacial landscapes: implications for the glacial history of northeastern Baffin Island, Arctic Canada. *Canadian Journal of Earth Sciences* **42**: 67–84.

Briner JP, Miller GH, Davis PT *et al.* 2006. Cosmogenic radionuclides from fiord landscapes support differential erosion by overriding ice sheets. *GSA Bulletin* **118**: 406–420.

Briner JP, Axford Y, Forman SL *et al.* 2007. Multiple generations of interglacial lake sediment preserved beneath the Laurentide Ice Sheet. *Geology* **35**: 887–890.

Cluett AA, Thomas EK. 2021. Summer warmth of the past six interglacials on Greenland. *Proceedings of the National Academy of Sciences* **118**: e2022916118.

Chappell J, Omura A, Esat T *et al.* 1996. Reconciliation of late Quaternary sea levels derived from coral terraces at Huon Peninsula with deep sea oxygen isotope records. *Earth Planetary Science Letters* **141**: 227–236.

Corbett LB, Bierman PR, Davis PT. 2016. Glacial history and landscape evolution of southern Cumberland Peninsula, Baffin Island, Canada, constrained by cosmogenic 10Be and 26Al. *GSA Bulletin* **128**: 1173–1192.

Crump SE, Fréchette B, Power M *et al.* 2021. Ancient plant DNA reveals High Arctic greening during the Last Interglacial. *PNAS* **118**: 13e2019069118.

Davis PT, Briner JP, Coulthard RD *et al.* 2006. Preservation of Arctic landscapes overridden by cold-based ice sheets. *Quaternary Research* **65**: 156–163.

de Vernal A, Hillaire-Marcel C. 2008. Natural variability of Greenland climate, vegetation, and ice volume during the past million years. *Science* **320**: 1622–1625.

Dyke AS, Andrews JT, Clark PU *et al.* 2002. The Laurentide and Innuitian ice sheets during the Last Glacial Maximum. *Quaternary Science Reviews* **21**: 9–31.

Dyke AS. 2004. An outline of North American deglaciation with emphasis on central and northern Canada. *Developments in Quaternary sciences* **2**: 373–424.

Farnsworth LB, Kelly MA, Bromley GRM *et al.* 2018. Holocene history of the Greenland Ice-Sheet margin in Northern Nunatarssuaq. *Northwest Greenland. Arktos* **4**: 1–27.

Feyling-Hanssen RW. 1976. The stratigraphy of the Quaternary Clyde Foreland Formation, Baffin Island, illustrated by the distribution of benthic foraminifera. *Boreas* **5**: 77–94.

Francis DR, Wolfe AP, Walker IR *et al.* 2006. Interglacial and Holocene temperature reconstructions based on midge remains in sediments of two lakes from Baffin Island, Nunavut, Arctic Canada. *Palaeogeography, Palaeoclimatology, Palaeoecology* **236**: 107–124.

Fréchette B. 2007. Palynologie de la Terre de Baffin et du Groenland: approches méthodologiques et reconstitutions climatiques du dernier interglaciaire et de l'Holocène. [Ph D thesis]. Montréal, Canada, Université du Québec à Montréal.

Fréchette B, de Vernal A, Richard PJH. 2008a. Holocene and Last Interglacial cloudiness in eastern Baffin Island, Arctic Canada. *Canadian Journal Earth Sciences* **45**: 1221–1234.

Fréchette B, de Vernal A, Guiot J *et al.* 2008b. Methodological basis for quantitative reconstruction of air temperature and sunshine from pollen assemblages in Arctic Canada and Greenland. *Quaternary Science Reviews* **27**: 1197–1216.

Fréchette B, Wolfe AP, Miller GH *et al.* 2006. Vegetation and climate of the last interglacial on Baffin Island, Arctic Canada. *Palaeogeography, Palaeoclimatology, Palaeoecology* **236**: 91–106.

Grant KM, Rohling EJ, Ramsey CB *et al.* 2004. Sea-level variability over five glacial cycles. *Nature communications* **5**: 1–9.

Joynt EH, Wolfe AP. 2001. Paleoenvironmental inference models from sediment diatom assemblages in Baffin Island lakes (Nunavut, Canada) and reconstructions of summer water temperature. *Canadian Journal of Fisheries and Aquatic Sciences* **58**: 1222–1243.

Kelly M, Funder S, Houmark-Nielsen M *et al.* 1999. Quaternary glacial and marine environmental history of northwest Greenland: a review and reappraisal. *Quaternary Science Reviews* **18**: 373–392.

Lamb HF. 1985. Palynological Evidence for Postglacial Change in the Position of Tree Limit in Labrador. *Ecological Monographs* **55**(2): 241–258.

Livingstone DM, Lotter AF, Walkery IR. 1999. The decrease in summer surface water temperature with altitude in Swiss Alpine lakes: a comparison with air temperature lapse rates. *Arctic, Antarctic, and Alpine Research* **31**: 341–352.

Løken OH. 1966. Baffin Island Refugia Older than 54,000 Years. *Science* **153**: 1378–1380.

Lozhkin AV, Anderson PM. 1995. The Last Interglaciation in Northeast Siberia. *Quaternary Research* **43**: 147–158.

McCulloch MT, Esat T. 2000. The Coral Record of Last Interglacial Sea Levels and Sea Surface Temperatures. *Chemical Geology* **169**: 107–29.

McFarlin JM, Axford Y, Osburn MR *et al.* 2018. Pronounced summer warming in northwest Greenland during the Holocene and Last Interglacial. *PNAS* **115**: 6357–6362.

Melles M, Brigham-Grette J, Minyuk PS *et al.* 2012. 2.8 Million Years of Arctic Climate Change from Lake El'gygytgyn, NE Russia. *Science* **337**: 315–320.

Meyer-Jacob C, Vogel H, Boxberg F *et al.* 2014. Independent measurement of biogenic silica in sediments by FTIR spectroscopy and PLS regression. *Journal of Paleolimnology* **52**: 245–255.

Michelutti N, Simonetti A, Briner JP *et al.* 2009. Temporal trends of pollution Pb and other metals in east-central Baffin Island inferred from lake sediment geochemistry. *Science Total Environment* **407**: 5653–5662.

Miller GH, Mode WN, Wolfe AP *et al.* 1999. Stratified interglacial lacustrine sediments from Baffin Island, Arctic Canada: chronology and paleoenvironmental implications. *Quaternary Science Reviews* **18**: 789–810.

Miller GH, Wolfe AP, Steig EJ *et al.* 2002. The Goldilocks dilemma: big ice, little ice, or "just-right" ice in the Eastern Canadian Arctic. *Quaternary Science Reviews* **21**: 33–48.

Miller GH, Wolfe AP, Briner JP *et al.* 2005. Holocene glaciation and climate evolution of Baffin Island, Arctic Canada. *Quaternary Science Reviews* **24**: 1703–1721.

Mode WN. 1980. *Quaternary stratigraphy and palynology of the Clyde Foreland. Baffin Island, NWT, Canada* [Ph D thesis]. Boulder, University of Colorado Boulder.

Myers-Smith IH, Kerby JT, Phoenix GK *et al.* 2020. Complexity revealed in the greening of the Arctic. *Nature Climate Change* **10**: 106–117.

Nelson AR. 1982. Aminostratigraphy of Quaternary marine and glaciomarine sediments, Qivitu Peninsula, Baffin Island. *Canadian Journal of Earth Sciences* **19**(5): 945–961.

Pendleton SL. 2018. *Holocene Glacier Fluctuations and Quaternary Ice Sheet Evolution on Cumberland Peninsula, Baffin Island*. University of Colorado: Boulder.

Refsnider KA, Miller GH, Fréchette B *et al.* 2013. A chronological framework for the Clyde Foreland Formation, Eastern Canadian Arctic, derived from amino acid racemization and cosmogenic radionuclides. *Quaternary Geochronology* **16**: 21–34.

Richard PJH, Bouchard MA, Gangloff P. 1991. The significance of pollen-rich inorganic lake sediments in the Cratère du Nouveau-Québec area, Ungava, Canada. *Boreas* **20**: 135–149.

Short SK, Nichols H. 1977. Holocene pollen diagrams from subarctic Labrador-Ungava: vegetational history and climatic change. *Arctic Alpine Research* **9**: 265–290.

Steig EJ, Wolfe AP, Miller GH. 1998. Wisconsinan refugia and the glacial history of eastern Baffin Island, Arctic Canada: Coupled evidence from cosmogenic isotopes and lake sediments. *Geology* **26**: 835–838.

Sugden DE. 1978. Glacial Erosion by the Laurentide Ice Sheet. *Journal of Glaciology* **20**: 367–391.

Thomas EK, Axford Y, Briner JP. 2008. Rapid 20th century environmental change on northeastern Baffin Island, Arctic Canada inferred from a multi-proxy lacustrine record. *Journal of Paleolimnology* **40**: 507–517.

Thomas EK, Briner JP. 2009. Climate of the past millennium inferred from varved proglacial lake sediments on northeast Baffin Island, Arctic Canada. *Journal of Paleolimnology* **41**: 209–224.

Waelbroeck C, Labeyrie L, Michel E *et al.* 2002. Sea-Level and Deep Water Temperature Changes Derived from Benthic Foraminifera Isotopic Records. *Quaternary Science Reviews* **21**: 295–305.

Wilson CR, Michelutti N, Cooke CA *et al.* 2012. Arctic lake ontogeny across multiple interglaciations. *Quaternary Science Reviews* **31**: 112–126.

Wolfe AP. 1994. Late Wisconsinan and Holocene diatom stratigraphy from Amarok Lake, Baffin Island, N.W.T., Canada. *Journal of Paleolimnology* **10**: 129–139.

Wolfe AP, Fréchette B, Richard PJH *et al.* 2000. Paleoecology of a >90,000-year lacustrine sequence from Fog Lake, Baffin Island, Arctic Canada. *Quaternary Science Reviews* **19**: 1677–1699.

Wolfe AP, Miller GH, Olsen CA *et al.* 2004. Geochronology of high latitude lake sediments. In *Long-Term Environmental Change in Arctic and Antarctic Lakes. Developments in Paleoenvironmental Research*, Pienitz R, Douglas MSV, Smol JP (eds). **8**. Springer: Dordrecht; 19–52.